C.P. No. 981

C.P. No. 981

MINISTRY OF TECHNOLOGY

AERONAUTICAL RESEARCH COUNCIL

CURRENT PAPERS

A Survey of the Infrared Radiation Properties of Carbon Dioxide

By

J. P. Hodgson

LONDON: HER MAJESTY'S STATIONERY OFFICE

1968

Price 15s. 6d. net

C.P. No. 981*

December, 1966

A survey of the infrared radiation properties of carbon dioxide

by

J. P. Hodgson
Department of the Mechanics of Fluids
University of Manchester

SUMMARY

This paper consists of a survey of theoretical and experimental approaches to the prediction of the low resolution emissivity of an infrared band of a polyatomic molecule. Spectral band models and molecular models are discussed, with carbon dioxide being taken as an example of such a molecule.

---

*Replaces A.R.C. 28 645

List of Contents

Introduction

Like solids, gases can emit, absorb and transmit radiation according to the elementary laws of radiation. The emission or absorption spectrum of

a gas is not continuous but is distributed into bands containing many single spectral lines caused by well-defined quantum number changes within the gas molecule.

Except in the presence of external electric or magnetic fields there are three types of quantised transitions to be considered. These are:

1. rotational transitions
2. vibrational transitions, and
3. electronic transitions.

For a typical molecule the change of internal energy ΔE, for the individual transition increases down this list. That is,

$$\Delta E_1 << \Delta E_2 << \Delta E_3$$

Thus one particular type of transition dominates the energy change in a general transition in which several quantum number changes are involved, and the bands are named accordingly:

1. rotational bands, typically in the wavelength range 10^2 to 10^4 microns,

2. vibrational bands, typically in the wavelength range 1 to 30 microns, and

3. electronic bands, typically in the wavelength range 10^{-2} to 1 micron.

It should be noted that electronic bands contain an electronic transition, which defines the spectral position of the band, and also vibrational and rotational transitions which cause a large number of different spectral lines to be formed close to the positions defined by the electronic transition. Similarly for a vibrational band, a change in vibrational quantum number defines the spectral position whereas the actual lines of the band are caused by simultaneous vibrational and rotational transitions. For this reason vibrational bands are often referred to as "vibration-rotation" bands.

The actual position of a band of course depends entirely on the size, shape and internal forces of the molecule concerned.

Here we are concerned entirely with vibration-rotation bands under low spectroscopic resolution. For any given polyatomic molecule there are many vibration-rotation bands, each one accompanied by a particular change in vibrational quantum number(s). Under low resolution the rotational lines of the band are not distinguished and the overall effect of these lines is to broaden the band.

The spectral properties of the carbon dioxide molecule are reviewed together with the calculation of the integrated band intensity of absorption and the spectral emissivity. Radiation laws and some useful parameters are defined and a survey of spectral band models is given. The 4.3 micron band of carbon dioxide is the band of greatest interest here, but the arguments can be extended to apply to other bands of the carbon dioxide molecule and to bands of other molecules.

1(a) Einstein Coefficients in a System of Two-Level Particles

The basis of the method involves the solution of the time-dependent Schrodinger equation in the presence of a perturbation potential.

To understand the physics of the problem let us consider a simple system of molecules each of which can be in either of two states, with energies E_u and E_ℓ, where $E_u > E_\ell$.

The respective populations of these states, N_u and N_ℓ, at a temperature T are related by the Boltzmann distribution function so that

$$\frac{g_\ell}{N_\ell} e^{-\frac{E_\ell}{kT}} = \frac{g_u}{N_u} e^{-\frac{E_u}{kT}} , \qquad (1.1)$$

where g_u and g_ℓ are the degeneracies of the states and 'k' is Boltzmann's constant. This can be rewritten

$$\frac{N_\ell}{N_u} = \frac{g_\ell}{g_u} e^{\frac{h\nu_{u\ell}}{kT}} \qquad (1.2)$$

where $E_u - E_\ell = h\nu_{u\ell}$ defines $\nu_{u\ell}$. These equations describe the equilibrium population of the system, but if for some reason the equilibrium is disturbed (for example by a sudden decrease in surrounding temperature), the above equations no longer apply and there will be a redistribution of population, restoring equilibrium. (In the particular example quoted, molecules with energy E_u will decay by radiation of a photon into state E_ℓ until the above equations hold again at the new temperature. Molecular collisions are not considered, internal dynamic equilibrium being re-established by radiative transfer only).

We now consider the above system to be enclosed in unit volume and subject to a spectral radiation field of density ρ_ν until the whole system has reached equilibrium. There will be three main processes going on, each one characterized by an Einstein Coefficient(1).

Spontaneous Emission

The higher energy molecules decay so that the number of transitions is given by

$$N_u \; A_{u\ell} \quad \text{per cm}^3 \quad \text{per sec.}$$

where $A_{u\ell}$ is the Einstein Coefficient for spontaneous emission.

Induced Emission and Absorption

The molecules are also subject to interactions with the radiation field and a collision with a photon of energy $(E_u - E_\ell)$ can induce a change of state in either direction, such that the number of upward transitions is given by

$$N_\ell \; B_{\ell u} \rho_{\nu u\ell} - N_u \; B_{u\ell} \rho_{\nu u\ell} \text{ per cm}^3 \text{ per sec},$$

where $B_{\ell u}$ is the Einstein Coefficient for absorption, and $B_{u\ell}$ is the Einstein Coefficient for induced emission. Usually we have $N_\ell >> N_u$ and absorption dominates induced emission, but if $N_u >> N_\ell$ the situation can be used for light amplification (LASER) provided $A_{u\ell}$ is not too large.

Since the system is in equilibrium

$$N_u \; A_{u\ell} = N_\ell \; B_{\ell u} \rho_{\nu u\ell} - N_u \; B_{u\ell} \rho_{\nu u\ell} \tag{1.3}$$

and it follows that

$$\frac{N_\ell}{N_u} = \frac{A_{u\ell} + B_{u\ell} \rho_{\nu u\ell}}{B_{\ell u} \rho_{\nu u\ell}} = \frac{g_\ell}{g_u} \; e^{\frac{h\nu_{u\ell}}{kT}} \tag{1.4}$$

For black body radiation systems in equilibrium at the temperature T,

$$\rho_{\nu u\ell} = \frac{8\pi h \nu_{u\ell}^3}{c^3} \left(e^{\frac{h\nu_{u\ell}}{kT}} - 1\right)^{-1} \tag{1.5}$$

and it can be seen, by solving the second part of (1.4) for $\rho_{\nu u\ell}$ and comparing with (1.5) that the Einstein Coefficients are inter-related. In fact

$$g_\ell \; B_{\ell u} = g_u \; B_{u\ell} \quad ,$$
$$A_{u\ell} = \frac{8\pi h \nu_{u\ell}^3}{c^3} B_{u\ell} \quad .$$

(b) Radiation Density, Emissivity and Integrated Absorption

Radiation density $\rho_\nu(T)$ is defined as the radiant energy per unit frequency interval at frequency ν. The velocity of propagation is the velocity of light 'c' and by using the arguments of kinetic theory we can show that the isotropic radiant energy, incident in time dt, on area of wall dA, in frequency interval ν to $\nu + d\nu$ is

$$\tfrac{1}{4} \; c \; \rho_\nu(T) \; d\nu dA \; dt.$$

It follows from Kirchhoff's Law that the radiant energy emitted from area dA of a non-black body at a specified temperature in time dt into a solid angle of 2π and in frequency range ν to $\nu + d\nu$ is

$$\varepsilon_\nu(T) R_\nu^{o}(T)\, dA dt d\nu = \tfrac{1}{4} c\, \rho_\nu(T)\, dA dt d\nu, \tag{1.6}$$

where $R_\nu^{o}(T)$ is the Planck blackbody function (15) and $\varepsilon_\nu(T)$ is defined as the hemispherical spectral emissivity.

The effect of absorption by a sample of gas on which radiation is incident can be described for a collimated beam by the spectral absorption coefficient per unit length in the gas, $K_{L,\nu}$, which is defined by the relation

$$-d\rho_\nu d\nu = \rho_\nu K_{L,\nu} dL\, d\nu, \tag{1.7}$$

which states that the net decrease in radiation density is proportional to the incident radiation density and the path length 'L' of the radiation in the gas. The constant of proportionality is the spectral absorption coefficient. The path length dL is traversed in time (dL/c), therefore for an incident radiation density of $\rho_\nu(T)$ the radiation energy lost per unit time is $-c \frac{d\rho_\nu}{dL} d\nu$, and so the number of induced transitions from energy level E_ℓ to level E_u, due to radiation in the range ν to $\nu + d\nu$, is

$$-\frac{c}{h\nu} d\rho_\nu d\nu \qquad \text{per unit time.}$$

Therefore the total number of transitions per unit time is given by

$$N_{tr} = \int_{\Delta\nu_{u\ell}} \frac{c\rho_\nu K_{L,\nu}}{h\nu} d\nu, \tag{1.8}$$

where $\Delta\nu_{u\ell}$ indicates integration over the line width at frequency $\nu_{u\ell}$. If the spectral line is very narrow and ρ_ν does not change much across it then

$$N_{tr} \simeq \frac{c\rho_{\nu u\ell}}{h\nu_{u\ell}} \int_{\Delta\nu_{u\ell}} K_{L,\nu} d\nu \tag{1.9}$$

Induced emission is coherent with the incident radiation, and this expression can be equated to the difference in numbers of induced transitions u to ℓ and ℓ to u. In terms of Einstein Coefficients this gives

$$N_{tr} = (N_\ell B_{\ell u} - N_u B_{u\ell})\rho_{\nu \ell u}. \tag{1.10}$$

Absorption coefficients of gases under normal circumstances are proportional to particle density and so we define the integrated line absorption (1) as the integral of the spectral absorption divided by pressure 'p' and wave velocity 'c'

$$\text{i.e.} \qquad S_{\ell u} = \frac{1}{pc} \int_{\Delta\nu_{u\ell}} K_{L,\nu} d\nu \qquad (1.11)$$

We see from (1.9) and (1.10) and (1.2) and(1.5)

$$S_{\ell u} = \frac{1}{pc} \cdot \frac{h\nu_{u\ell}}{c\rho_{\nu u\ell}} N_{tr}$$

$$= \frac{h\nu_{u\ell}}{pc^2} (N_\ell B_{\ell u} - N_u B_{u\ell})$$

$$= \frac{h\nu_{u\ell}}{pc^2} N_\ell B_{\ell u} \left(1 - \frac{N_u B_{u\ell}}{N_\ell B_{\ell u}}\right)$$

$$= \frac{h\nu_{u\ell}}{pc^2} N_\ell B_{\ell u} \left(1 - e^{-\frac{h\nu_{u\ell}}{kT}}\right),$$

$$\text{i.e.} \qquad S_{\ell u} = \frac{h\nu_{u\ell}}{pc^2} N_\ell B_{\ell u} \left(1 - e^{-\frac{h\nu_{u\ell}}{kT}}\right), \qquad (1.12)$$

$$\text{or} \qquad S_{\ell u} = \frac{c}{8\pi\nu_{u\ell}^2} \left(\frac{N_\ell}{p}\right) A_{u\ell} \frac{g_u}{g_\ell} \left(1 - e^{-\frac{h\nu_{u\ell}}{kT}}\right).$$

$S_{\ell u}$ is usually measured in units of $(\text{atmospheres})^{-1} \times (\text{centimetres})^{-2}$.

The value of the integrated line absorption gives us a measure of the brightness of a spectral line, and is a function of temperature.

The statement that absorption coefficients are proportional to pressure is not quite true since they are really proportional to density and only proportional to pressure at a fixed temperature. This method of standardization is common in gas dynamics, and it would be better to use the standard density unit, the amagat, except that we normally measure pressures rather than densities. In what follows, the units for optical path length will be taken as pressure times geometric path length, and the units for integrated line intensity will be $(\text{atmospheres})^{-1}$ $(\text{centimetres})^{-2}$ as stated above. This step is taken only to fall in line with previous work, which makes data correlation easier, although it would be physically more correct to say

$$S_{\ell u} = \frac{1}{\rho c} \int_{\Delta\nu_{u\ell}} K_{L,\nu} \, d\nu \qquad \text{(amagat)}^{-1} \text{ cm.}^{-2}$$

The picture so far enables us to calculate the line intensity for a transition provided that we can calculate the Einstein Coefficients. The quantity $S_{\ell u}$ is independent of the line shape which is given by $K_{L,\nu}$. We shall find that when applied to carbon dioxide the suffices l and u embrace several quantum numbers, since the upper and lower states have degeneracies. We shall then sum $S_{\ell u}$ over appropriate quantum numbers to give us the integrated band absorption.

We now give an abbreviated account of the quantum mechanical method of determining the Einstein Coefficients.

1 (c) Quantum Mechanical Method for Determining the Einstein Coefficients

This is a perturbation method (2,3), the validity of which is based upon the assumption that the radiation Hamiltonian has only a small effect on the unperturbed state of the system.

The Schrodinger equation may be written

$$H\psi = i\hbar \frac{\partial \psi}{\partial t} , \tag{1.13}$$

where H is the total Hamiltonian operator. We can represent H by $H = H^{o} + H'$, where H^{o} is the equilibrium Hamiltonian operator and H' the perturbed Hamiltonian operator. If H' is zero the solutions of the equation

$$H^{o}\psi = i\hbar \frac{\partial \psi}{\partial t} \tag{1.14}$$

are $\psi = \psi_n^{\,o}$, and $\psi_n^{\,o}$ represents a complete set of wave functions which can be expressed as

$$\psi_n^{\,o}(q, t) = \psi_n^{\,o}(q)\, e^{-\frac{iE_n t}{\hbar}} ,$$

where E_n is the energy of the state $\psi_n^{\,o}$. For H' non-zero the equation becomes

$$(H^{o} + H')\psi = i\hbar \frac{\partial \psi}{\partial t} , \tag{1.15}$$

and to obtain a solution we write $\psi = \sum_n c_n(t)\psi_n^{\,o}(q,t)$ and substitute

into the equation above giving:

$$\sum_n H^o c_n(t)\psi_n^o(q,t) + \sum_n H' c_n(t)\,\psi_n^o(q,t)$$

$$= i\hbar \sum_n \frac{dc}{dt}n\,\psi_n^o(q,t) + i\hbar \sum_n c_n(t)\,\frac{\partial\psi}{\partial t}n^o \qquad (1.16)$$

But (1.14) tells us that the first and last terms here are equal, so that

$$\sum_n H' c_n(t)\,\psi_n^o(q,t) = i\hbar \sum_n \frac{dc}{dt}n\;\psi_n^o(q,t). \qquad (1.17)$$

$|c_n(t)|^2$ is the fractional concentration of $\psi_n^o(q,t)$ in the state $\psi(q,t)$.

To obtain the rate of change of concentration of each state we multiply (1.17) by ψ_m^{o*} and integrate over all space,

$$\text{i.e.}\quad i\hbar \int \psi_m^{o*} \sum_n \frac{dc}{dt}n\;\psi_n^o\,d\tau = \int \psi_m^{o*} \sum_n H' c_n(t)\,\psi_n^o d\tau \qquad (1.18)$$

Since ψ_n^o represents a complete set $\int \psi_m^{o*}\,\psi_n^o\,d\tau = \delta mn$. Therefore we have left

$$\frac{dc}{dt}m = \sum_n \frac{1}{i\hbar}\,c_n \int \psi_m^{o*}\,H'\psi_n^o\,d\tau \qquad (1.19)$$

This last equation has no physical application as it stands, but the integral on the right is related to the probability of a change from state m to state n due to the presence of the perturbation Hamiltonian.

It can be shown that for a radiation field the Hamiltonian H' has the form (1)

$$H' = \sum_j \frac{ie_j\hbar}{m_j c}\;\underline{A}\cdot\nabla_j \qquad (1.20)$$

where e_j is the charge of the jth particle, with mass m_j and $\underline{A}$ is the vector magnetic potential of the radiation.

First consider a light wave polarised in the x-direction and

travelling in the z-direction; for this wave $A_2 = A_3 = 0$ and

$$A_1 = A_1^{o} \cos 2\pi\nu \left(t - {}^{z}/_{c}\right),$$

where A_1^{o} is a constant.

Substituting the expression for H_1' into the integral of equation (1.19) we get

$$\int \psi_m^{o*} \sum_j \frac{ie\hbar}{m_j c} A_{1,j} \frac{d}{dx_j} \psi_n^{o} \, d\tau$$

For visible and infrared radiation the wavelength is very much greater than the molecular dimensions, so that $A_{1,j}$ will be a constant in the region of the molecule, i.e. $A_{1,j} = A_1$ and then

$$\int \psi_m^{o*} H_1' \psi_n^{o} \, d\tau = \frac{i\hbar A_1}{c} e^{-\frac{i(E_m - E_n)t}{\hbar}} \times \sum_j \frac{e_j}{m_j} \int \psi_m^{o*} \frac{d}{dx_j} \psi_n^{o} \, d\tau \qquad (1.21)$$

If we consider the time-independent wave equations for the two states ψ_n^{o} and ψ_m^{o} we can show that

$$\int \psi_m^{o*} \frac{d}{dx_j} \psi_n^{o} d\tau = -\frac{m_j}{\hbar^2}(E_m - E_n) \int \psi_m^{o*} x_j \psi_n^{o} \, d\tau \qquad (1.22)$$

so that (1.21) reduces to

$$\int \psi_m^{o*} H_1' \psi_n^{o} d\tau = -\frac{i}{\hbar c} A_1 (E_m - E_n) e^{-\left(\frac{i(E_m - E_n)t}{\hbar}\right)} X_{mn} \qquad (1.23)$$

where

$$X_{mn} = \int \psi_m^{o*} \sum_j e_j x_j \psi_n^{o} d\tau \qquad (1.24)$$

That is, through the transformation (1.22) the integral in (1.19) becomes a

function of X_{mn}, the square of which represents the x-component of the molecular dipole moment matrix element (4) for a transition between the two states m and n. (1.19) reduces to

$$\frac{dc_m}{dt} = -\frac{A_1}{c\hbar^2} \sum_n c_n(E_m - E_n)\, e^{-\frac{i(E_m - E_n)t}{\hbar}}\, X_{mn}, \qquad (1.25)$$

for the physical system in which we have a fractional concentration of the mth state at t = 0 of $c_m(0) = \delta mn$. For perturbations from the initial state it follows that

$$\frac{dc_m}{dt} = -\frac{A_1}{c\hbar^2} X_{mn} (E_m - E_n)\, e^{-\frac{i(E_m - E_n)t}{\hbar}} \qquad (1.26)$$

Also for light of frequency ν at z = 0, A_1 becomes

$$A_1 = A_1^{\,o} \left[e^{2\pi i\nu t} + e^{-2\pi i\nu t}\right]$$

whence,

$$\frac{dc_m}{dt} = -\frac{A_1^{\,o}}{2c\hbar^2} X_{mn} (E_m - E_n)$$

$$\times \left[e^{\frac{i(E_m - E_n + h\nu)t}{\hbar}} + e^{\frac{i(E_m - E_n - h\nu)t}{\hbar}}\right] \qquad (1.27)$$

Integrate from ($t = 0$ to $t = t$
($c_m = 0$ to $c_m = c_m(t)$, then

$$c_m = \frac{i}{2c\hbar} A_1^{\,o} X_{mn}(E_m - E_n)$$

$$\times \left[\frac{e^{\frac{i(E_m - E_n + h\nu)t}{\hbar}} - 1}{E_m - E_n + h\nu} + \frac{e^{\frac{i(E_m - E_n - h\nu)t}{\hbar}} - 1}{E_m - E_n - h\nu}\right] \qquad (1.28)$$

which is large only for $E_m - E_n = \pm h\nu$, in all other cases the expression in brackets is of order unity. If we take $E_m > E_n$, then we can have only $E_m - E_n = +h\nu$ and the first term is never large.

The probability that the system will be in a state m after a time t

is therefore

$$\int c_m^* c_m \psi_m^{o*} \psi_n^{o} d\tau = \overline{c_m^* c_m} \div \frac{t^2}{4c^2\hbar^4} |A_1^o|^2 |X_{mn}|^2 (E_m - E_n)^2 \times \int_0^\infty \frac{\sin^2\left[\frac{(E_m - E_n - h\nu)t}{2\hbar}\right] d\nu}{(E_m - E_n - h\nu)^2 t^2/4\hbar^2} \tag{1.29}$$

This leads to

$$|c_m(t)|^2 = \frac{\pi^2 \nu_{mn}^2}{c^2\hbar^2} |A_1^o(\nu_{mn})|^2 |X_{mn}|^2 \cdot t \tag{1.30}$$

So far we have considered light fully polarized in the x-direction. For randomly polarized light, the cross terms vanish and we have left

$$|c_m(t)|^2 = \frac{\pi^2 \nu_{mn}^2}{c^2\hbar^2} \left[|A_1^o|^2 |X_{mn}|^2 + |A_2^o|^2 |Y_{mn}|^2 + |A_3^o|^2 |Z_{mn}|^2 \right] \tag{1.31}$$

where $|Y_{mn}|^2$ and $|Z_{mn}|^2$ are the y, z components of the electric dipole matrix elements and A_2^o, A_3^o the respective constant amplitudes of the incident radiation. For isotropic radiation $|A_1^o|^2 = |A_2^o|^2 = |A_3^o|^2 = \frac{1}{3}|\underline{A}^o|^2$, so that

$$|c_m(t)|^2 = \frac{\pi^2 \nu_{mn}^2}{3c^2\hbar^2} |\underline{A}^o|^2 |R_{mn}|^2 t, \tag{1.32}$$

where $|R_{mn}|^2 = |X_{mn}|^2 + |Y_{mn}|^2 + |Z_{mn}|^2$ is the square of the modulus of the total electric dipole matrix element

$$|R_{mn}|^2 = \left| \int \psi_m^{o*} \sum_j e_j \underline{q}_j \psi_n^{o} d\tau \right|^2 \tag{1.33}$$

We can relate $|\underline{A}^o(\nu_{mn})|^2$ to the radiation density, since

$$\underline{A} = \underline{A}^{o} \sin (2\pi\nu_{mn} t)$$

and $$\underline{E} = -\frac{1}{c}\frac{\partial \underline{A}}{\partial t}$$, where $\underline{E}$ is the electric field,

$$= -\frac{2\pi\nu_{mn}}{c} \underline{A}^{o} \cos (2\pi\nu_{mn} t);$$

therefore $$\overline{|\underline{E}|^2} = \frac{2\pi^2 \nu_{mn}^2}{c^2} |\underline{A}^{o}|^2$$

$$= 4\pi\rho_{\nu mn},$$

therefore $$\rho_{\nu mn} = \frac{\pi\nu_{mn}^2}{2c^2} |\underline{A}^{o}|^2 ,$$

so that $$|c_m(t)|^2 = \frac{2\pi}{3\hbar^2} \rho_{\nu mn} |R_{mn}|^2 t.$$

Now $|c_m(t)|^2 / t$ is the probability per unit time that a molecule of the system will undergo a transition to state m from state n under the influence of the radiation density $\rho_{\nu mn}$, where $E_m > E_n$. It follows from (1.3) that the number of upward transitions per unit time is

$$N_n \frac{|c_m(t)|^2}{t} = N_n B_{nm} \rho_{\nu nm} ,$$

Therefore

$$B_{nm} = \frac{|c_m(t)|^2}{\rho_{\nu mn} t}$$

$$= \frac{2\pi}{3\hbar^2} |R_{mn}|^2 \qquad (1.34)$$

and $$A_{mn} = \frac{64\pi^4 \nu_{mn}^3}{3\hbar c^3} \frac{g_n}{g_m} |R_{mn}|^2 .$$

Hence we have succeeded in relating the Einstein Coefficients to the sum of the squares of the matrix elements of the dipole moment components which can be evaluated for any physical system if ALL the wave functions are known. This last condition is the overriding one.

So far we have shown that the integrated line absorption due to a

transition from a state with quantum number n to a state with quantum number m is given by

$$S_{nm} = \frac{8\pi^3 \nu_{mn}}{3\hbar c^2} \left(\frac{N_n}{p}\right) |R_{mn}|^2 \left(1 - e^{-\frac{h\nu_{mn}}{kT}}\right). \qquad (1.35)$$

The wave functions and selection rules for diatomic molecules will now be briefly discussed, and developed later to apply to the carbon dioxide molecule.

2(a) Matrix Elements and Selection Rules for Diatomic Molecules

For a diatomic molecule the Schrodinger time-independent equation can be solved in the harmonic approximation (1,5). The resulting wave functions govern the transitions that can take place when a molecule is subjected to a perturbing radiation field. This leads to selection rules. We consider now the one-dimensional harmonic oscillator.

The complete time-independent wave functions for the one-dimensional harmonic oscillator are the orthonormal Hermite polynomials

$$\psi_n(x) = \left[\left(\frac{\alpha}{\pi}\right)^{\frac{1}{2}} \frac{1}{2^n n!} \right]^{\frac{1}{2}} H_n(\sqrt{\alpha}\, x) e^{-\frac{\alpha x^2}{2}} \qquad (2.1)$$

where $x = r - r_e$ is the displacement from the equilibrium internuclear distance and α is related to the potential energy 'V' through

$$V(x) = \frac{\alpha^2 x^2 h^2}{2m_r} \quad ,$$

where m_r is the reduced mass of the molecule. The energy levels are given by

$$E_n = (n+\tfrac{1}{2})h\nu_o .$$

In the dipole approximation we can represent the electric moment μ by

$$\mu = \mu_o + \mu_1(r - r_e) = \mu_o + \mu_1 x,$$

where μ_o is the permanent dipole moment of the molecule, and μ_1 is induced by the departure from equilibrium. If we now calculate the matrix element X_{mn} for a change of state due to a perturbing radiation field, we find that

$$X_{n,n} = \mu_0 , \tag{2.2a}$$

producing no change of state, and

$$\left.\begin{aligned} X_{n,n+1} &= \mu_1\sqrt{\frac{n+1}{2\alpha}} \\ X_{n,n-1} &= \mu_1\sqrt{\frac{n}{2\alpha}} \end{aligned}\right\} \tag{2.2b}$$

For all other values of $m \neq n,\ n \pm 1$ we find $X_{nm} = 0$, leading us to the selection rule in the harmonic approximation of $\Delta n = \pm 1$. It is the value of μ_1 which we have difficulty in finding and the point at which we need further empirical information. Later (Section 3) it will be seen that we can solve the problem fairly satisfactorily.

The method now adopted is to proceed to find the matrix elements and the line intensities, which we expect to contain constant factors of proportionality related to the magnitudes of the dipole moments. We consider the vibrational levels to be degenerate due to the total rotational increments of angular momentum and also due to the orientation of this angular momentum in space. The former give rise to the rotational quantum number K which can have non-negative integral values and the latter give rise to the magnetic quantum number M, which can have (2K + 1) values extending from -K to +K.

We consider the integrated line absorption (defined in (1.12) and also called the 'line intensity' or 'line strength')due to a change of state from (n K M) to (n' K' M') (see page 8) where the changes in quantum numbers are governed by the selection rules of the harmonic oscillator and rigid rotator.

Thus $|R_{nm}|^2$ becomes $|R_{nKM \to n'K'M'}|^2$.

The selection rules limiting K and M are, for

x,y polarized light $\Delta M = \pm 1, \quad \Delta K = \pm 1,$

z polarized light, $\Delta M = 0, \quad \Delta K = \pm 1.$

Using this information we can sum over all possible transitions for a vibration quantum number change of n to n', and hence calculate $|R_{n\to n'}|^2$ and $\alpha_{nn'}$, the vibrational band intensity. This method, due to Herman (6,7) is now described briefly.

Let the jth component of the matrix element given in (1.33) be

$$|R_{nm}|_j \equiv |R_{nKM \to n'K'M'}|_j$$

$$= \left| \int \psi^*_{nKM} \, \mu_j(r, \theta, \zeta) \, \psi_{n'K'M'} d\tau \right| ,$$

where $\mu_j(r, \theta, \zeta)$ is the jth component of the electric dipole moment vector $\underline{\mu}(r, \theta, \zeta)$. ψ_{nKM} is the complete time-independent wave function of the diatomic molecule, which we can separate into the form

$$\psi_{nKM} = S_{nK}(r) \, g_{KM}(\theta, \zeta),$$

and we can also write $\mu_j(r, \theta, \zeta) = \mu(r) \, F_j(\theta, \zeta)$. We can now sum $|R_{nKM \to n'K'M'}|^2$ over all transitions in which the selection rules are obeyed. For the summation over M M' and components j we have

$$|R_{nK \to n'K'}|^2 = \sum_{M \, M'} |R_{nKM \to n'K'M'}|^2$$

$$= \left| \int S^*_{nK} \mu(r) \, S_{n'K'} d\tau \right|^2$$

$$\times \sum_{MM'} \sum_j \left| \int g^*_{KM} \, f_j(\theta, \zeta) g_{K'M'} d\tau \right|^2 \qquad (2.3)$$

and it can be shown (11) that the summation on the right is given by

$$(K\delta_{K-1, \, K'} + (K+1) \, \delta_{K+1, K'}),$$

where δ_{mn} is the Kronecker δ-function.

Corresponding to the matrix element $|R_{nKM \to n'K'M'}|^2$ we have an integrated line absorption

$$S_{nKM \to n'K'M'} = \frac{8\pi^3}{3\hbar c^2} \, \frac{N_{nKM}}{p} \, \nu_{(nKM, \, n'K'M')}$$

$$\times \left[1 - e^{-\frac{h\nu_{(nKM, \, n'K'M')}}{kT}} \right] |R_{nKM \to n'K'M'}|^2 \qquad (2.4)$$

In the absence of magnetic fields the levels are degenerate due to the inability of the magnetic quantum number to split the levels, and this degeneracy is σ_{nK} (= (2K+1) for the state n, K) and so

$$N_{nKM} = \frac{N_{nK}}{\sigma_{nK}} \quad .$$

Therefore

$$S_{nK\to n'K'} = \frac{8\pi^3}{3hc} \frac{N_{nK}}{P} \nu(nK,n'K') \frac{1}{2K+1}$$

$$\times \left(1 - e^{-\frac{h\nu(nK,\, n'K')}{kT}}\right) \times \left| \int S^*_{nK}\, \mu(r)\, S_{n'K'} d\tau \right|^2$$

$$\times \left[K\delta_{K-1,K} + (K+1)\delta_{K+1,K'}\right] \quad . \qquad (2.5)$$

The values of the integral can be calculated in the harmonic approximation but contain the unknown factor due to the magnitude of the dipole moment vector; of this experimental knowledge is indeed very limited.

By a similar summation over KK' we can estimate the total vibrational band intensity(∝). However, this is more difficult than the summation over M since there is a variation in frequency over the band width. The result is

$$\alpha_{n\to n'} = \sum_{KK'} S_{nK\to n'K'}$$

$$= \frac{8\pi^3}{3hc^2} \frac{N_n}{P} \overline{\nu}_{n,n'} |R_{n\to n'}|^2 \left(1 - e^{-\frac{h\overline{\nu}_{n,n'}}{kT}}\right), \qquad (2.6)$$

where $\overline{\nu}_{n,n'}$ is a complicated function of the average frequency in the band, Owing to the approximation of complete harmonicity the values of n, n' are limited to being small and so the formulae can only be expected to hold at low temperatures and even then we can only find the relative band strength. Thus even if we know the band strength at room temperature, it is difficult to get a reasonable value for the band strength at much higher temperatures, since the harmonic approximation is no longer valid.

Before applying the above method to the carbon dioxide molecule it is necessary to know more about this molecule and its modes of vibration. The method (given in Section5) will be that formulated by Malkmus, which assumes a band intensity at room temperature and an average line width, with a given temperature variation.

2 (b) The Carbon Dioxide Molecule and its Infrared Spectrum (5,9)

The molecule has three atoms and therefore nine degrees of freedom. We can divide these into internal motion and external motion of the molecule as a whole.

(1) The external motion consists of translation of the molecule as a whole in the three orthogonal directions and, since the molecule is linear, the rotation of the molecule about the two axes perpendicular to the axis of the molecule.

(2) The internal motion consists of three modes of vibration and one of rotation which only becomes effective when one of the vibrational modes is excited.

By a linear transformation we can reduce the internal motion of the molecule to its normal co-ordinates, (x, y, z, q).

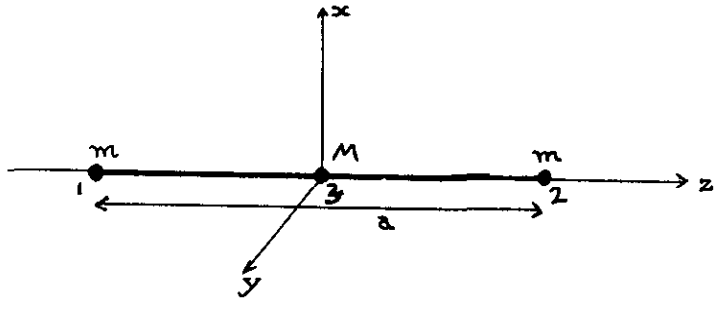

The kinetic energy is then given by

$$T = \tfrac{1}{2} m\dot{q}^2 + \tfrac{1}{2}\mu(\dot{x}^2 + \dot{y}^2 + \dot{z}^2)$$

where $q = (z_2 - z_1) - a$, $x = x_3 - \tfrac{1}{2}(x_1 + x_2)$,

$$y = y_3 - \tfrac{1}{2}(y_1 + y_2), \quad z = z_3 - \tfrac{1}{2}(z_1 + z_2), \qquad (2.7)$$

$$r^2 = x^2 + y^2, \; x = r\cos\phi, \; y = r\sin\phi,$$

and $$\mu = \frac{2Mm}{M + 2m}$$

This reduction to normal co-ordinates depends on the assumption that the vibrational amplitude is very much smaller than the inter-atomic separation.

To the harmonic approximation the potential energy is

$$V = V^{o} = \pi^2 m\nu_1^2 q^2 + 2\pi^2 \nu_2^2 \mu(x^2 + y^2) + 2\pi^2 \nu_3^2 \mu z^2. \qquad (2.8)$$

The solution of Schrodinger's equation for this potential leads us to the vibrational wave function

$$\psi^{n_1 n_2 n_3 \ell} = \psi^{n_1}(\sigma)\psi^{n_3}(\xi)\, R^{n_2 \ell}(\rho)\, e^{\pm i\ell\psi} \qquad (2.9)$$

where the non-dimensional quantities σ, ξ, ρ $\propto$ q, z, r respectively, $\psi^{n_1}(\sigma)$ and $\psi^{n_3}(\xi)$ are orthogonal Hermitian functions and $R^{n_2 \ell}(\rho) = \rho^{\ell} e^{-\rho^2/2} \sum_{K=0}^{n_2 - \ell} a_K \rho^K$.

Also, the total internal energy of the molecule (to the harmonic approximation) is

$$W^{n_1 n_2 n_3} = (n_1 + \tfrac{1}{2})\, h\nu_1 + (n_2 + 1)\, h\nu_2 + (n_3 + \tfrac{1}{2}) h\nu_3, \qquad (2.10)$$

so there are three fundamental vibration bands in which each of (n_1, n_2, n_3) changes by one unit.

The fundamental modes of vibration and the significance of the quantum numbers are demonstrated below (Table 1). The vibrational temperatures, frequencies and wave lengths are also given (10).

It can be seen that in the symmetric stretching mode there will be no change in dipole moment of the molecule, so that the matrix elements are all zero. This band is not observed in the infrared spectrum of carbon dioxide but only in the Raman spectrum. It does however combine with the other two modes giving rise to combination bands in the spectrum.

Table 1.

wave-length (μ)	wave-number cm^{-1}	$\theta_\nu = \frac{h\nu}{k}{}_{o_K}$	Type of mode.				Quantum number:
15	667	959	bending	↑ •	↓	↑ •	n_2
7·5	1336	1920	symmetric stretching	←•	•	•→	n_1
4·3	2349	3350	asymmetric stretching	•→	←•	•→	n_3

The quantum number 'ℓ', associated with the bending mode, is a measure of the angular momentum about an axis parallel to the ground state axis of the molecule. Thus 'ℓ' must be zero whenever the bending mode is unexcited, and it is found that the values that 'ℓ' can take are $n_2, (n_2 - 2), (n_2 - 4)$ ..... 1 or 0. This mode of vibration introduces an asymmetry into the molecule about the ground state axis of the molecule, so that the dipole moment matrix element is non-zero and furthermore the change of dipole moment is perpendicular to the axis of the molecule. This characterises the type of band spectra emitted by changes of quantum number n_2. Only such bands are observed for which (9)

Δn_2 is ODD, $\Delta \ell = \pm 1$ and Δn_3 is EVEN.

The asymmetric stretching mode has asymmetry parallel to the axis of the molecule so that a change of quantum number n_3 causes a dipole moment change parallel to the molecular axis, which produces a characteristic "parallel band" spectrum. Only such bands are found for which

Δn_2 is EVEN, $\Delta \ell = 0$, Δn_3 is ODD.

To avoid confusion as to the values that Δn_2 and Δn_3 can have, it is as well to note that in the harmonic approximation the selection rules demand that $\Delta n_2 = \pm 1$, $\Delta n_3 = 0$ for a perpendicular band and $\Delta n_2 = 0$, $\Delta n_3 = \pm 1$ for a parallel band. All other quantal jumps are forbidden, but ONLY in the harmonic approximation. In practice the potential energy wells of the molecule contain much anharmonicity and this increases the possibility of quantal steps exceeding the harmonic restriction of $\Delta n = \pm 1$, especially for large values of n. However, it should be pointed out that the probability of a change in quantum numbers rapidly decreases with increasing magnitudes of the change. Thus we can readily accept a violation of the selection rule $\Delta n = \pm 1$, though the band spectra produced by changes of $\Delta n > 1$ are of a much weaker intensity. Therefore in the above restrictions on Δn_2 and Δn_3, for the most probable transitions read zero for even and one for odd.

The selection rules governing changes in 'ℓ' are much more rigorous since the rigid rotator model is a better approximation to rotational motion than the harmonic approximation is to vibrational motion.

The above discussion can be verified by applying a small perturbation to the harmonic potential and calculating the transition probabilities from the resulting perturbed wave functions. The two statements on Δn_2, $\Delta \ell$ and Δn_3 are the result of this work (9) and the value of Δn_1 is shown to be of no significance here.

To realize what these results mean consider the spectral bands that appear at the frequencies

$\Delta n_1 \nu_1 + \Delta n_2 \nu_2 + \Delta n_3 \nu_3$ (Δn's are of course integral).

Only such bands are found for which $(\Delta n_2 + \Delta n_3)$ is an ODD number, as we have seen.

(i) For Δn_2 odd dipole moment change is perpendicular to the molecular axis.

(ii) For Δn_3 odd dipole moment change is parallel to the molecular axis.

These restrictions have an important effect on the spectrum of the carbon dioxide molecule, in particular in the formation of combination bands. Consider the transitions leading to the two observed bands:

$$1. \quad \nu' = \Delta n_1' \nu_1 + \Delta n_2' \nu_2 + \Delta n_3' \nu_3 \tag{2.11}$$

$$2. \quad \nu'' = \Delta n_1'' \nu_1 + \Delta n_2'' \nu_2 + \Delta n_3'' \nu_3 \tag{2.12}$$

A combination band would be

$$3. \quad (\nu' + \nu'') = (\Delta n_1' + \Delta n_1'')\nu_1 + (\Delta n_2' + \Delta n_2'')\nu_2 + (\Delta n_3' + \Delta n_3'')\nu_3 \tag{2.13}$$

Since bands 1 and 2 are observed both $(\Delta n_2' + \Delta n_3')$ and $(\Delta n_2'' + \Delta n_3'')$ must be odd; therefore $(\Delta n_2' + \Delta n_2'') + (\Delta n_3' + \Delta n_3'')$ must be even, so that a combination band of two observed bands cannot be observed. However, the asymmetric mode often interacts with the other two modes producing observed bands, since Δn_1 is unlimited; for example,

$$\nu = \nu_1 + \nu_2 \qquad 00^{\circ}0 \leftrightarrow 11^{1}0$$

$$\nu = \nu_1 + \nu_3 \qquad 00^{\circ}0 \leftrightarrow 10^{\circ}1$$

We have seen that we can predict the positions of the various bands knowing the three fundamental frequencies, and we shall now investigate the structure of the bands which will be found to be of two main types (5). In order to do this we shall need to consider the rotational motion more closely.

By choosing axes (ξ, η, ζ) to be along the principal axes of the molecule we can ensure that the Hamiltonian will depend only upon the principal moments of inertia (A, B, C). Let A,B be the two equal moments of inertia and let the linear molecular axis lie along ζ with moment of inertia C. (The following analysis applies to any triatomic molecule).

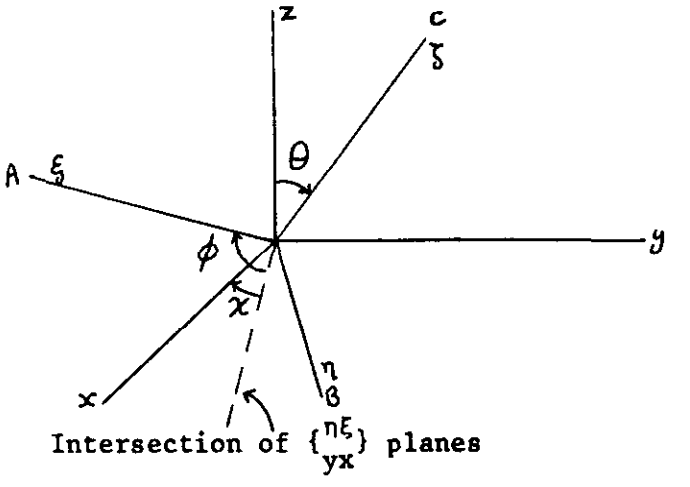

The orientation may be described by the three Eulerian angles (θ, ϕ, χ). After forming the Hamiltonian and Schrodinger's equation for $V \equiv 0$, we can separate variables and solve for the wave functions

$$\Psi = \Theta(\theta)\, e^{iK\phi}\, e^{iM\chi}$$

where K and M are integers, in order that Ψ be single-valued. From the resulting equation for $\Theta(\theta)$ we can show that the energy levels are defined by

$$W^{JK} = \frac{J(J+1)}{2A} + \left(\frac{1}{C} - \frac{1}{A}\right)\frac{K^2\hbar^2}{A} \qquad (2.14)$$

where J is a positive integer. The relationships, given by the equation, between J, M and K suggest their physical significance. These relations are

$$J \geq |K| \ , \quad \text{if} \quad |K| \geq |M| \ ,$$

$$J \geq |M| \ , \quad \text{if} \quad |M| \geq |K| \ ,$$

i.e. J. is greater than or equal to the larger of the magnitudes of the two quantum numbers K and M. On the other hand we may say that for fixed values of J, there is a limit on the values of M and K, such that

$$|K| \leq J \qquad \text{and} \qquad |M| \leq J \ .$$

This suggests that J, K, M can be interpreted as representing angular momentum quantum numbers, and it can be shown that angular momentum is given as follows:

the total angular momentum L is given by $L = J(J+1)\hbar^2$,

the component along the ζ axis by $L_\zeta = K\hbar$,

the component along the z axis by $L_z = M\hbar$.

From the formulae restricting certain values of M,K it can be shown that the degeneracies of the states of angular momentum (J,K) are given by

$$g_{JK} = 2J + 1 \qquad K = 0,$$

$$= 2(2J + 1) \qquad K > 0, \text{ etc.}$$

Selection rules can be found by determining the matrix elements representing the direction cosines ρ_{ij}. The results are the rules $J = \pm 1, 0$; $K = 0$; $M = \pm 1, 0$, for which $\rho_{\zeta x}$, $\rho_{\zeta y}$ and $\rho_{\zeta z}$ have matrix elements differing from zero, and $\Delta J = \pm 1, 0$; $\Delta K = \pm 1$; $\Delta M = \pm 1, 0$ for which $\rho_{\eta x}$, $\rho_{\eta y}$, $\rho_{\eta z}$ and $\rho_{\xi x}$, $\rho_{\xi y}$, $\rho_{\xi z}$ have finite values of matrix elements.

Assuming the above expressions for the degeneracy and that the total intensity of radiation from a state is proportional to the degeneracy of that state, we can find the relative intensity of the rotational lines in the vibrational band.

The above two sets of selection rules lead to two types of band, called parallel and perpendicular according to the direction in which the change of dipole moment occurs with respect to the molecular axis. This corresponds to the change in quantum number K, which can be 0 or ± 1.

(i) Selection rules $\Delta J = \pm 1, 0$ and $\Delta K = 0$,

Reference to the energy constant W^{JK} for this molecule shows that the lines of an absorption band will be given by the expressions in the following table, where ν_o is the normal frequency of vibration. The intensities of the lines in the three branches corresponding to $\Delta J = -1, 0, +1$, are also given (5)

$$\text{- ve branch:} \quad \nu^{J,K}_{J-1} = \nu_o - \frac{\hbar J}{2\pi A} \; ; \; I^J_{J-1} = \mathcal{A} \sum_{K \neq 0}^{J-1} Q \frac{J^2-K^2}{4J} \; e^{-\sigma(J^2+J)-\beta\sigma K^2} \tag{2.15}$$

$$0 \quad \text{branch:} \quad \nu^{JK}_{JK} = \nu_o \; ; \; I = \mathcal{A} \sum_{J=1}^{\infty} \sum_{K=0}^{J} K^2 \frac{2J+1}{2J(J+1)} \; e^{-\sigma(J^2+J)-\beta\sigma K^2} \tag{2.16}$$

$$\text{+ ve branch:} \quad \nu^{J-1,K}_{J,K} = \nu_o + \frac{\hbar J}{2\pi A} \; ; \; I^J_{J-1} = \mathcal{A} \sum_{K=0}^{J-1} Q \frac{J^2-K^2}{4J} \; e^{-\sigma(J^2-J)-\beta\sigma K^2} \tag{2.17}$$

where $\mathcal{A}$ is a constant depending on the molecular dipole moment matrix elements; Q = 1,2 where K = 0 or $\neq$ 0, $\sigma = \frac{\pi^2}{2AKT}$ and $\beta = \frac{A}{C} - 1$.

So far this discussion of the parallel band has been for a general triatomic molecule, but for a linear molecule, such as carbon dioxide, vibrating in the asymmetric stretching mode, the rotational motion is like that of a symmetric rotator. The moment of inertia C tends to zero, so that β becomes infinite. However, since C is so near to zero the quantum number K cannot have any meaning, except when it is zero. The immediate consequences of this is that the zero branch vanishes and the intensities are represented by the much simplified expressions:

$$I^{J}_{J-1} = \tfrac{1}{4}\mathcal{A}\,J\;e^{-\sigma(J^2+J)} \tag{2.18}$$

$$I^{J-1}_{J} = \tfrac{1}{4}\mathcal{A}\,J\;e^{-\sigma(J^2-J)} \tag{2.19}$$

which are seen to be very similar to the intensity variations of the vibration-rotation band of a diatomic molecule. The intensity variation is a direct function of σ but the form of the band depends little on its value. Since, when ℓ is non-zero, the molecule loses some of its symmetry, we have twice as many lines in a band for $\ell>0$, as well as a weak central branch. In fact in the band for $\ell = 0$, these lines are superposed in pairs, the lines with odd values of J being absent. The moment of inertia C becomes finite as in a general triatomic molecule, if $\ell>0$. Fig. 1 should help to clarify this point.

(ii) Selection rules $\Delta J = \pm 1,0$ and $\Delta K = 0$.

Again reference to the energy level constant W^{JK} will give us the line structure of a general triatomic perpendicular band, which is more complicated than the parallel band. The general appearance depends greatly on the ratio (A/C), which is infinite for CO_2 in a state with $\ell = 0$, but it is useful to look at the case for which $\ell>0$, i.e. (A/C) finite. This band can be described by a series of superimposed single bands, two sets of which are given for values of $\Delta K = \pm 1$, and each single band has positive, zero and negative branches. The frequencies of the lines of the Kth single band on the negative side of ν_o are given by:

$$\text{- branch: } \nu^{J,K}_{J-1,K-1} = \nu_o - \frac{\pi}{2\pi A}\left[J + \beta(K-\tfrac{1}{2})\right],\quad J = K,\ K+1\ \ldots. \tag{2.20}$$

$$\text{O branch: } \nu^{J,K}_{J,K-1} = \nu_o - \frac{\pi}{2\pi A}\,\beta(K-\tfrac{1}{2}) \tag{2.21}$$

$$+ \text{ branch: } \quad \nu^{J-1\ K}_{J,\ K-1} = \nu_o - \frac{\hbar}{2\pi A}\left[-J + (K-\tfrac{1}{2})\right], J = K+1, K+2, \ldots \qquad (2.22)$$

Note that the allowed values of J start with K and K + 1, not zero, following the structure rule J≥K. The intensities are given by expressions similar to those for a parallel band.

The overall picture of the band for a value of (A/C) = 5 and $\sigma = 0.018$ for the vibrational transition 00^00 to 01^10 can then be built up as shown in Fig. 1 (d). Single bands are shown for values of K up to three.

In the special case of the moment of inertia C approaching zero the central zero bands of all the single bands move to the frequency ν_o and so the resulting picture is as in Fig. 1(e)., with a very strong central part of the band.

For a perfectly harmonically designed molecule the actual band would consist of several of these bands (shown in Fig. 1(e).) exactly superimposed, there being more bands at higher temperatures. At the same frequency we would observe for example a superposition of the bands $01^10 \leftrightarrow 00^00$, $05^50 \leftrightarrow 04^40$, $33^31 \leftrightarrow 32^21$, ...

However, since in the real molecule the potential wells are of the Morse type the energy levels come closer together as the molecule moves towards dissociation, so that the frequency of the band emitted for the transition $05^50 \rightarrow 04^40$, say, is smaller than that emitted for $01^10 \rightarrow 00^00$. Thus in observing the emission of radiation with increasing temperature the vibration bands are seen to spread into regions of longer wavelength. To complicate the harmonic spectra still further the line spacing of the positive branch decreases and that of the negative branch increases as the quantum number increases, due to centrifugal stretching, (21), and Doppler broadening causes the spectral lines to spread into a continuous spectrum.

It is worthwhile to note that for CO_2 the frequency of the n_2 (bending) mode is very nearly half the frequency of the n_1 (symmetric stretching) mode. This leads to resonance and a good approximation can be made in calculating the intensities (see the method of Section 3(b) for intensity calculations in the 4.3μ region).

The effect of the shape of the blackbody radiation spectrum on the relative brightness of the vibration bands is shown diagrammatically in Fig. 2. Fig. 3 shows some absorption bands at room temperature, all of which are listed in Table 2 together with other important bands.

3(a) The Result of the Application of the Line Summation Method to the Calculation of the Total Relative Band Intensity of the Carbon Dioxide 4.3μ Band

Referring back to the expression for the line intensity for a diatomic molecule, we can calculate the equivalent expressions for the parallel band of carbon dioxide.

The line intensity given by the transition $(n_1\ n_2^{\ell}\ n_3 J \to n_1'\ n_2'^{\ell'}\ n_3'\ J')$ is

$$S(n_1 n_2^{\ell} n_3,\ J \to n_1' n_2'^{\ell'} n_3' J') = \frac{8\pi^3 N_T \nu}{3kc^2 Q_V' Q_R'}\ g_{J'\ell'}\ a_{J\ell}^{J'\ell'}\ |R n_1 n_2^{\ell} n_3 J \to n_1' n_2'^{\ell'} n_3' J'|^2$$

$$\times\ e^{-\frac{W_V' + W_R'}{kT}}\ \left(1 - e^{-\frac{h\nu}{kT}}\right), \qquad (3.1)$$

where ν = the frequency associated with the indicated change in quantum numbers,

$|R n_1 n_2^{\ell} n_3 J \to n_1' n_2'^{\ell'} n_3' J'|^2$ = the corresponding matrix element.

N_T = the total number of molecules per unit volume per unit pressure,

$g_{J'\ell'}$ = the degeneracy of the upper state, with rotational quantum number J',

Q_R' = the complete rotational partition function, with energy levels W_R',

Q_V' = the complete vibrational partition function, with energy levels W_V',

$a_{J\ell}^{J'\ell'}$ = the amplitude (5) factors corresponding to the rotational change of state $J\ \ell \to J'\ell'$; typically

$$a_{J\ell\pm1}^{J\ell} = \frac{(J \pm \ell)(J \mp \ell + 1)}{4J(J+1)} \qquad \text{for } \ell \neq 0.$$

To complete the calculation of the total band absorption we sum the above expression over all values of JJ' governed by the selection rules $\Delta J = 0, \pm 1$. (11). Physically this represents adding all the intensities of the lines in the band. The result is

$$\alpha(n_1 n_2^{\ell} n_3 \rightarrow n_1' n_2'^{\ell'} n_3') = \sum_{JJ'} S(n_1 n_2^{\ell} n_3 J \rightarrow n_1' n_2'^{\ell'} n_3' J')$$

$$= \frac{8\pi^3 N_T}{3hc^2 Q_V} \bar{\nu} g_{\ell} \beta^2 e^{-\frac{W_V}{kT}} (1 - e^{-\frac{h\bar{\nu}}{kT}}) , \qquad (3.2)$$

where g_{ℓ} = 1 for $\ell = 0$,
{
2 for $\ell \neq 0$,

$\bar{\nu}$ = the frequency of the absorption band centre,

$\beta^2 = |R n_1 n_2^{\ell} n_3; n_1' n_2'^{\ell'} n_3'|^2$, and

Q_V and W_V are given by

$$W_V'(n_1 n_2 n_3) + W_R'(\ell, J) = W_V(n_1 n_2 n_3 \ell) + W_R(J),$$

$$Q_V'(n_1 n_2 n_3) \; Q_R'(\ell, J) = Q_V(n_1 n_2 n_3 \ell) \; Q_R(J),$$

so that the summation over JJ' becomes easier. The expressions for W_V', Q_V', etc., will be given in the discussion of Malkmus's paper.

If $\Delta\ell = 0$, the above expression for the band absorption is correct, but if $\Delta\ell = \pm 1$, there are two possible final states to which the molecule can go and so the intensity of each band in this case will be half that for $\Delta\ell = 0$, but there will be twice as many lines since there are two separate transitions possible.

1.3 (b) A Special Method of Calculating the Partition Function of Carbon Dioxide in Application to the 4.3μ Infrared Band (13)

It will now be shown that the band absorptions for the various bands in the 4.3μ region can be related, using the harmonic approximation and an assumption concerning the frequencies of the fundamentals. The final formulae will be of use in predicting the total band strength of the 4.3μ band and will also give us information as to which transitions are most important.

(i) Calculation of the Partition Function

The asymmetric stretching mode in carbon dioxide has its levels of excitation classified by a change in the quantum number n_3. When the other two quantum numbers remain unchanged and n_3 changes by unity, emitting or absorbing a photon of radiation, the transition of states gives rise to the 4.3μ band.

The usual expression (10) for the vibrational energy levels of a linear triatomic molecule, taking into account the anharmonicity present, is

$$E(n_1n_2n_3\ell) = hc \Big[\omega_1(n_1 + \tfrac{1}{2}) + \omega_2(n_2 + 1) + \omega_3(n_3 + \tfrac{1}{2}) + x_{11}(n_1 + \tfrac{1}{2})^2 + x_{22}(n_2 + 1)^2 + x_{33}(n_3 + \tfrac{1}{2})^2 + g_{22}\ell^2 + x_{12}(n_1 + \tfrac{1}{2})(n_2 + 1) + x_{23}(n_2 + 1)(n_3 + \tfrac{1}{2}) + x_{13}(n_1 + \tfrac{1}{2})(n_3 + \tfrac{1}{2}) + \ldots \Big] \qquad (3.3)$$

where ω_1, ω_2, ω_3 are the wavenumbers of the fundamentals and the x_{ij} are anharmonic correction terms given by

$$x_{11} = -0.3,\ x_{22} = -1.3,\ x_{33} = -12.5, \qquad (\text{cm.}^{-1})$$

$$x_{12} = 5.7,\ x_{23} = -11.0,\ x_{13} = -21.9, \qquad (\text{cm.}^{-1})$$

and $g_{22} = 1.31$ cm.$^{-1}$.

The fundamental wavenumbers for this empirical formula are $\omega_1 = 1351.2$, $\omega_2 = 672.2$, $\omega_3 = 2396.4$ cm.$^{-1}$ It follows that for a transition in which $\Delta n_3 = 1$, the wavenumber involved is

$$\omega(n_1n_2n_3 1 \to n_1\ n_2\ (n_3 + 1)1) = \left(E(n_1n_2(n_3 + 1)1) - E(n_1n_2n_3 1)\right) \frac{1}{hc}$$

$$= \omega_3 + \tfrac{1}{2}x_{13} + x_{23} + 2x_{33} + x_{13}n_1 + x_{23}n_2 + 2x_{33}n_3 + \ldots. \qquad (3.4)$$

Now the fundamental wavenumber ω_1 is almost twice the fundamental wavenumber ω_2, and so the states which have the same values of $(2n_1 + n_2)$ and n_3 have very nearly the same energy (13). The states with the same

value of ℓ still perturb one another, and each pair of states would have to be studied separately, leading to a mammoth task. The alternative is to group the two quantum numbers n_1 and n_2 into a new quantum number

$$n = 2n_1 + n_2 \quad ,$$

and to define a wavenumber $\bar{\omega}$ such that

$$\bar{\omega} = \tfrac{1}{2}(\tfrac{1}{2}\omega_1 + \omega_2).$$

We also note that $2x_{23} = x_{13}$ to a good approximation, so that if we define

$$\bar{x} = \tfrac{1}{2}(\tfrac{1}{2}x_{13} + x_{23})$$

we have $$\bar{x}n = x_{13}n_1 + x_{23}n_2$$

and $$\bar{\omega}n = \omega_1 n_1 + \omega_2 n_2.$$

The transition wavenumber then becomes

$$\omega_{nn_3} = (nn_3 \rightarrow nn_3 + 1)$$

$$= \omega_3 + \tfrac{1}{2}x_{13} + x_{13} + x_{23} + 2x_{33} + \bar{x}n + 2x_{33}n_3 \qquad (3.5)$$

Also the energy of any level relative to the ground state is in the harmonic approximation:

$$E(n_1, n_2, n_3, \ell) = \omega_1 n_1 + \omega_2 n_2 + \omega_3 n_3.$$

This becomes $E(n, n_3) = \bar{\omega}n + \omega_3 n_3$.

The vibrational partition function is given by

$$Q_V(T) = \sum_{n_1=0}^{\infty} \sum_{n_2=0}^{\infty} \sum_{n_3=0}^{\infty} \sum_{\ell=\{0}^{n_2} {}_{1} \; g_\ell \, e^{-\frac{E(n_1 n_2 n_3)}{kT}} \quad , \qquad (3.6)$$

where the degeneracy g_ℓ, dependent on ℓ, has the values

$$g_\ell = \begin{cases} 1, & \ell = 0, \\ 2, & \ell > 0. \end{cases}$$

We can separate out the partition function due to asymmetric stretching, this is

$$Q_3(T) = \sum_{n_3=0}^{\infty} e^{-\frac{n_3\omega_3 hc}{kT}} = (1 - e^{-\frac{\omega_3 hc}{kT}})^{-1} \qquad (3.7)$$

The remaining partition function is

$$Q_o(T) = \sum_{n_1=0}^{\infty} \sum_{n_2=0}^{\infty} \sum_{\ell=\begin{cases}0\\1\end{cases}}^{n_2} g_\ell e^{-\frac{(\omega_1 n_1+\omega_2 n_2)hc}{kT}} . \qquad (3.8)$$

We can now change the order of summation, so that after summing over ℓ, we sum over all values of n_1 and n_2 such that $2n_1 + n_2 = n$, and then sum over all values of n.

Let $\sum^{n^*} f(n_1 n_2 \ell)$ denote the summation over ℓ (even or odd) followed by the summation over all values of n_1 and n_2 such that $2n_1+n_2 = n$ (n even or odd), i.e.

$$\left.\begin{aligned} \sum^{n^*} f(n_1 n_2 \ell) &= \sum_{\text{even } n_2=0}^{n} \sum_{\text{even } \ell=0}^{n_2} f\left[\tfrac{1}{2}(n-n_2),\ n_2, \ell\right] && n \text{ even} \\ &= \sum_{\text{odd } n_2=1}^{n} \sum_{\text{odd } \ell=1}^{n_2} f\left[\tfrac{1}{2}(n_1-n_2),\ n_2 \ell\right] && n \text{ odd} \end{aligned}\right\} \qquad (3.9)$$

Then, since $\omega_1 n_1 + \omega_2 n_2 = \bar{\omega} n$, the partition function is given by

$$Q_o(T) = \sum_{n=0}^{\infty} \sum^{n^*} g_\ell e^{-\frac{\bar{\omega} n hc}{kT}}$$

$$= \sum_{n=0}^{\infty} \left[e^{-\frac{n\bar{\omega} hc}{kT}} \left(\sum^{n^*} g_\ell\right)\right] . \qquad (3.10)$$

The two summations are quite straightformward and are accomplished by treating ℓ and n odd and even separately. The result is (13)

$$Q_o(T) = (1 - e^{-\frac{\bar{\omega}hc}{kT}})^{-3} \quad (1 + e^{-\frac{\bar{\omega}hc}{kT}})^{-1}$$

$$= (1 - e^{-\frac{2\bar{\omega}hc}{kT}})^{-1} \quad (1 - e^{-\frac{\bar{\omega}hc}{kT}})^{-2} \qquad (3.11)$$

which can be seen to be the harmonic oscillator approximation partition function obtained by replacing ω_1 by $2\bar{\omega}$ and ω_2 by $\bar{\omega}$. Obviously we could have put $\frac{1}{2}\omega_1 \simeq \omega_2 \simeq \bar{\omega}$ straight into the harmonic approximation to derive this result, but since the bands for which n is constant fall very close to each other in the spectrum, we can predict these individual band intensities much more easily using the above formulation.

In the 4.3μ band $\Delta n_1 = \Delta n_2 = 0$, and so $\Delta\ell = 0$ also. So the integrated absorption coefficient is given by (3.2), that is:

$$\alpha(n_1 n_2 n_3 \ell \rightarrow n_1' n_2' n_3' \ell') = \frac{8\pi^3}{3hc} N_T \beta^2 \omega' g_\ell e^{-\frac{E(n_1 n_2 n_3 \ell)}{kT}}$$

$$\times \frac{1}{Q_V} \left[1 - e^{-\frac{\omega' hc}{kT}}\right] \quad ,$$

where ω' is the wavenumber of the band centre. For a transition which involves only the quantum number change $|\Delta n_3| = 1$, we can show that $\beta^2 \propto (n_3 + 1)$ in the harmonic approximation (as in the case of a diatomic molecule in Section 2 (a)).

We can now sum the integrated absorption coefficient over all values of ℓ, n_1 and n_2, such that $2n_1 + n_2 = n$, and we shall derive the integrated absorption coefficient for the group of bands for which n is a constant and n_3 changes by unity, that is

$$\alpha_{nn_3}(T) = \sum^{n^*} \alpha(n_1 n_2 n_3 \ell \rightarrow n_1 n_2 n_3 + 1\ell). \qquad (3.12)$$

In order to determine the relative intensities of these bands we need also the fractional population $N^{nn3}(T)$ of the level for which $2n_1 + n_2 = n$ and n_3 are fixed. This is

$$N^{nn3}(T) = \frac{g^n e^{-\frac{nhc\bar{\omega}}{kT}} \quad e^{-\frac{n_3 hc\omega_3}{kT}}}{Q_V(T)} \qquad (3.13)$$

where g^n is the degeneracy of the state for which n=constant, and $g^n = \sum_{\ell}^{n^*} g_\ell = \begin{cases} \frac{1}{4}(n+2)^2 & n \text{ even}, \\ \frac{1}{4}(n+1)(n+3) & n \text{ odd}. \end{cases}$ (3.14)

Thus,

$$N^{nn3}(T) = g^n \; e^{-\frac{n\bar{\omega}hc}{kT}} \; e^{-\frac{n_3\omega_3 hc}{kT}} \times \left[1 - e^{-\frac{\bar{\omega}hc}{kT}}\right]^3 \left[1 + e^{-\frac{\bar{\omega}hc}{kT}}\right] \left[1 - e^{-\frac{\omega_3 hc}{kT}}\right] . \quad (3.15)$$

The fractional population of some of the lower vibrational states defined by the 4 internal quantum numbers n_1, n_2, n_3, ℓ, is shown in Fig. 4. (14)

It follows that we can estimate the relative intensities of the band groups:

$$\frac{\alpha_{no}(T)}{\alpha_{oo}(T)} = (\sum_{\ell}^{n^*} g_\ell) e^{-\frac{n\bar{\omega}hc}{kT}} = g^n e^{-\frac{n\bar{\omega}hc}{kT}} = \frac{N^{no}(T)}{N^{oo}(T)} ,$$

and

$$\frac{\alpha_{nn_3}(T)}{\alpha_{no}(T)} = (n_3 + 1) e^{-\frac{n_3\omega_3 hc}{kT}} = (n_3+1) \frac{N^{nn3}(T)}{N^{no}(T)} ,$$

so that $\frac{\alpha_{nn_3}(T)}{\alpha_{oo}(T)} = (n_3 + 1) \frac{N^{nn3}(T)}{N^{oo}(T)} = (n_3 + 1) g^n \; e^{-\frac{(n\bar{\omega} + n_3\omega_3)hc}{kT}}$ (3.16)

For a perfect gas at ordinary pressures; $N_T \propto 1/T$ and

$$\alpha_{no}(T) \propto \frac{1}{T} \; N^{no}(T) \; (1 - e^{-\frac{\omega_3 hc}{kT}}) .$$

Therefore,

$$\frac{\alpha_{nn_3}(T)}{\alpha_{nn_3}(T_o)} = \frac{T_o}{T} \cdot \frac{N^{nn3}(T)}{N^{nn3}(T_o)} \cdot \frac{1 - e^{-\frac{\omega_3 hc}{kT}}}{1 - e^{-\frac{\omega_3 hc}{kT_o}}} , \quad (3.17)$$

for a given reference temperature T_o. Thus, we can find $\frac{\alpha_{nn_3}(T)}{\alpha_{nn_3}(T_o)}$ for all n, n_3 and hence the overall absolute band strength if we know $\alpha_{oo}(T_o)$. At T_o the intensity we observe is

$$\sum_{n=0}^{\infty} \sum_{n_2=0}^{\infty} \alpha_{nn_3}(T_o) = \alpha_{oo}(T_o) \sum_{n=0}^{\infty} \sum_{n_3=0}^{\infty} \frac{\alpha_{nn_3}(T_o)}{\alpha_{oo}(T_o)}$$

$$= \alpha_{oo}(T_o) \left(\sum_{n=0}^{\infty} g^n e^{-\frac{n\bar{\omega}hc}{kT_o}} \right) \left(\sum_{n_3=0}^{\infty} (n_3 + 1) e^{-\frac{n_3\omega_3 hc}{kT_o}} \right)$$

$$= \alpha_{oo}(T_o)\, Q_o(T_o) \sum_{n_3=0}^{\infty} (n_3 + 1)\, e^{-\frac{n_3\omega_3 hc}{kT_o}} \quad .$$

The summation over n_3 can be shown to be given by

$$\sum_{n_3=0}^{\infty} (n_3+1) e^{-\frac{n_3\omega_3 hc}{kT_o}} = Q_3(T_o) \left[1 - (1 - e^{-\frac{\omega_3 hc}{kT_o}}) e^{-\frac{\omega_3 hc}{kT_o}} \ln(1-e^{-\frac{\omega_3 hc}{kT_o}}) \right] ,$$

which can be calculated. The integrated band intensity of absorption at temperature T_o will be given by

$$\sum_{n=0}^{\infty} \sum_{n_3=0}^{\infty} \alpha_{nn_3}(T_o) = \alpha_{oo}(T_o) Q_V(T_o) \left[1 - (1 - e^{-\frac{\omega_3 hc}{kT_o}}) e^{-\frac{\omega_3 hc}{kT_o}} \ln(1 - e^{-\frac{\omega_3 hc}{kT_o}}) \right] \qquad (3.18)$$

Thus one measurement of absorption at room temperature enables us to calculate $\alpha_{oo}(T_o)$, from which we can find the integrated band intensity at all temperatures, using the formulae of this section.

The work of Penner (1), after derivation of (3.2) consists of comparing the ratios of β^2 and of $\alpha(n_1 n_2^{\ell} n_3 \rightarrow n_1' n_2'^{\ell'} n_3')$ for the ν_2-fundamental and the combination transition

$$(n_1, n_2, {}^{\ell} n_3 \rightarrow (n_1 + 1), (n_2 + 1)^{\ell+1}, n_3).$$

1.4(a) Radiation Laws and Definitions

In (1.6) the relationship between hemispherical spectral emissivity, radiation density and the spectral radiancy for the surface of an opaque solid was given. We may define the hemispherical spectral emissivity of an opaque solid surface as the ratio of the spectral radiance which it emits into solid angle 2π to the spectral radiancy of a blackbody at the same temperature,

i.e.

$$\varepsilon_{\omega} = \frac{R_{\omega}(T)}{R^{o}_{\omega}(T)} \quad , \tag{4.1}$$

where $R^{o}_{\omega}(T)$ is the Planck blackbody radiation function (15) based on wave number. It can be shown that the absorbed spectral radiant energy per unit area is equal to the emitted spectral radiant energy per unit area if the surface is in thermal equilibrium with the radiation. This amounts to saying

$$\alpha_{\omega}(T) = \varepsilon_{\omega}(T) \qquad \text{(Kirchhoff's Law (16))}, \tag{4.2}$$

where $\alpha_{\omega}(T)$ is the spectral absorptivity.

Kirchhoff's Law in this form applies also to non-opaque substances (1), except that both α_{ω} and ε_{ω} must be evaluated for the same thickness. It follows that if P_{ω} is the spectral attenuation per unit area in the radiation per unit opical path length, the emissivity of optical path length dX is given by

$$\varepsilon_{\omega}(T) = P_{\omega}(T)dX, \text{ where } X=pl \text{ (atm.cm.)}$$

or

$$R_{\omega} = R^{o}_{\omega} P_{\omega} dX. \tag{4.3}$$

i.e. The spectral radiancy of any substance equals the product of the spectral absorptivity and the spectral radiancy of a blackbody.

Consider now the optical system of a "slab" of gas with optical thickness $X_o = pl$, as in Fig. 5. The change in transmitted radiation occurring in a depth dX is due to:

(i) the emitted spectral radiancy in dX, $P_\omega(T_g)d\lambda R^o_\omega(T_g)$;

(ii) the attenuation due to absorbers in dX, $P_\omega(T_g)dXR_\omega(X)$.

The net increase in radiant power moving from left to right in Fig. 5 is therefore

$$dR_\omega(X) = R_\omega(X + dX) - R_\omega(X)$$

$$= \left[R^o_\omega(T_g) - R_\omega(X)\right] \cdot P_\omega(T_g)\, dX,$$

Leading to the result that

$$R_\omega(X_o) = R^o_\omega(T_g)\left(1 - e^{-P_\omega(T_g)X_o}\right) + R_\omega(0)e^{-P_\omega(T_g)X_o} \qquad (4.4)$$

where $R_\omega(0)$ is the incident radiation from a light source, say.

It follows directly from this equation that if there is no change in spectral radiancy through the gas i.e. $R_\omega(X_o) = R_\omega(0)$ we have

$$R_\omega(0) = R_\omega(X_o) = R^o_\omega(T_g).$$

Since $R^o_\omega(T)$ is a single-valued function it follows that the (monochromatic) temperature of the radiation is equal to the temperature of the gas. This situation is used to determine temperature in line-reversal technique, about which more will be said later.

If there is no incident radiation, i.e. $R_\omega(0) = 0$, The resulting expression defines the spectral emissivity of a volume of gas

$$\varepsilon_\omega = 1 - e^{-P_\omega X_o}$$

The total energy radiated by the gas at a temperature T is given by

$$\int_0^\infty R^o_\omega \left[1 - e^{-P_\omega X_o}\right] d_\omega = \varepsilon\, \sigma\, T^4, \qquad (4.5)$$

where σ is Stefan's constant and ε is the total hemispherical emissivity.

The spectral radiancy of a black body is a single-valued function of temperature. Since in practice there are no black bodies it is useful to define the brightness temperature of a body, which is a function of the wave number and of the geometric position with respect to the source and surrounding media. Between a source and a point of observation there is usually a region of absorbing medium which causes spectral attenuation $P_\omega X$,

If the source has a hemispherical spectral emissivity $\mathcal{E}_\omega(T)$ and temperature T_o, the observed spectral radiancy is

$$R^o_\omega(T_o) \cdot \varepsilon_\omega(T_o) e^{-P_\omega(T_p)X} \cdot \frac{d\Omega}{2\pi} \, d\omega ,$$

where T_p is the temperature of the absorbing material and $d\Omega$ is the solid angle subtended at the source by a detector at the point of observation; d_ω is the wavenumber interval observed at wave number ω. If the source was a perfect black-body and there was no absorption of radiation between the source and detector, the same spectral radiancy would be observed at the point of interest, for a body temperature T_b, where

$$R^o_\omega(T_o)\varepsilon_\omega(T_o) e^{-P_\omega(T_p)X} \frac{d\Omega}{2\pi} \, d\omega = R^o_\omega(T_b) \frac{d\Omega}{2\pi} \, d\omega , \qquad (4.6)$$

T_b is called the brightness temperature of the body. Since ε_ω and $e^{-P_\omega X}$ are less than one it follows that $T_o > T_b$. The parameter $P_\omega(T)$ is called the spectral absorption and is related to the integrated absorption $S(T)$ by

$$\int_0^\infty P_\omega(T) \, d_\omega = S(T).$$

The absorption and emissivity of an isolated spectral line will now be studied and the usefulness of the various terms will become apparent. The procedure will be generalized to the case of many spectral lines in order that the properties of bands may be understood.

Spectral lines and line broadening (11).

Consider an atom or molecule in an excited state in translational equilibrium in a region containing similar particles. This individual particle can change its state, and internal energy, by several mechanisms.

(i) Absorption or emission of a photon without being simultaneously in contact with another particle

(ii) Absorption or emission of a photon during a collision with another particle

(iii) An upward change of state the energy for which is derived from the large kinetic energy of a collision with another molecule (inelastic collision).

(iv) A downward change of state during a collision accompanied by a corresponding increase in the kinetic energy of two particles (super-elastic collision).

(i) and (ii) are basically radiative transfer mechanisms while (iii) and (iv) are unaccompanied by any radiative features.

Which of the above mechanisms dominates depends on the state of the gas and the particular way the total energy is distributed between the various degrees of freedom. For example, (iii) dominates in the relaxation region of a shock wave while (ii), in the emission case, dominates when equilibrium has been reached behind a shock wave at a moderately high pressure.

Since we are interested in radiation properties of gases, (i) and (ii) will be of most importance here, but (iii) and (iv) can be investigated since the redistribution of states they cause influences the state of the gas and the mechanisms (i) and (ii).

Mechanisms (i) and (ii) are accompanied by observable radiation and for a given transition the photon of energy $h\nu_o$ involved can be detected. If we have a very large number of excited and de-excited particles in translational equilibrium with each other and with an energy source, a large number of transitions will take place. If only one transition is involved the energies of all the photons emitted and observed will be similar but not all exactly equal to $h\nu_o$ since there are in the main, three important phenomena which cause an energy spread among the quanta. These are

(a) Natural line broadening

(b) Collision, or pressure broadening, and

(c) Doppler line broadening.

(a) Natural line broadening is closely related to Heisenberg's uncertainty principle (2,11) which states that the product of the uncertainty of an energy state and the uncertainty in the time a particle is in that state has a minimum value given by

$$\Delta E_u \quad \Delta t \geq \hbar$$

If we consider a molecule in an upper energy state E_u with a constant probability per unit time of decaying (as inferred by (1.30), the uncertainty in the time that a molecule is in state E_u is the mean lifetime τ_u of that state. Thus the energy spread of the state is

$$\Delta E_u \geq \hbar / \tau_u .$$

Since we consider particles in equilibrium with radiation, particles in the lower state will be excited after a mean lifetime τ_ℓ in the lower state (on the average). The net effect is a spreading of the spectral line into a curve of well-known intensity distribution.

(b) Collision broadening. As the pressure of a gas increases so does the molecular collision rate which is accompanied by a corresponding increase in the number of collision-induced radiative transitions. This causes a reduction in the mean lifetime of all states causing further uncertainty in the energy of each level, broadening the spectral line still further.

(c) Doppler broadening. Consider a particle moving with a velocity v, emitting a photon in the direction of its motion. The observed frequency of the photon (ν) will be greater than that observed (ν_o) if the particle were at rest by an amount $\nu - \nu_o = \nu_o \frac{v}{c}$, where 'c' is the speed of light. Since in a gas there is a Maxwellian velocity distribution we shall observe a Maxwellian frequency distribution about a central mean.

These are the commonest phenomena which cause spectral line broadening in molecular spectra. The shape of the spectral lines in each case, being identical for types (a) and (b) is well-known. In general we can consider that (b) is pressure dependent and (c) is temperature dependent.

For a single spectral line with one type of broadening dominating, the function $P_\omega(T)$ has a definite form though its magnitudes vary according to the total strength of each spectral line. It follows that P_ω is not the most useful form for expressing the spectral absorption.

Since the line shapes are well-known, we define the normalized line shape parameter $b(\omega)$ which gives a measure of the relative intensity of each part of any line broadened by one of the usual phenomena so that

$$\int_0^\infty b(\omega)\, d\omega = 1 ,$$

The spectral absorption of a given line (under given broadening conditions) is then given by

$$P_\omega = S\, b(\omega) ,$$

and the emissivity is

$$\varepsilon_\omega = 1 - e^{-SX_o b(\omega)} .$$

(i) For natural and collision broadening (also known as Lorentz or contour broadening)

$$b(\omega) = \frac{\alpha_L}{\pi} \left[(\omega - \omega_o)^2 + \alpha_L^{\,2} \right]^{-1} , \qquad (4.7)$$

where ω_o is the wavenumber of the line centre and $\alpha_L = \alpha_L(p, T)$ is the Lorentz half-width at half-height of the line.

(2) For Doppler Broadening:

$$b(\omega) = \sqrt{\frac{\ln 2}{\pi}} \quad \frac{1}{\alpha_D} \; e^{-\frac{(\omega - \omega_o)^2 \ln 2}{\alpha_D^2}} \tag{4.8}$$

where $\alpha_D = \alpha_D(T)$ is the Doppler half-width at half-height.

The shape of the two lines is drawn in Fig. 6 for the same intensity and half-width and it can be seen that (b) tends to zero more rapidly that (a), and has a greater ratio of (height/width). Sometimes (b) can be approximated by the square line shape.

Consider now the total emission due to a single spectral line. This will be given by

$$\int_0^\infty R_\omega^o \varepsilon_\omega \, d\omega = \int_0^\infty R_\omega^o (1 - e^{-SXb(\omega)}) \, d\omega \tag{4.9}$$

If the emissivity were unity the total radiation would be

$$\int_0^\infty R_\omega^o \, d\omega = \sigma T^4 \qquad \text{(Stefan's Law)},$$

so that the total hemispherical emissivity of a line would be given by

$$\varepsilon_{line} = \frac{1}{\sigma T^4} \int_0^\infty R_\omega^o \, (1 - e^{-SXb(\omega)}) \, d\omega \tag{4.10}$$

Since R_ω^o is a slowly varying function it is practically constant across the spectral line at ω_o, so that

$$\varepsilon_{line} = \frac{R_{\omega o}^o}{\sigma T^4} \int_0^\infty (1 - e^{-SXb(\omega)}) \, d\omega \tag{4.11}$$

The integrand is close to zero except for a very small region $\Delta\omega_o$ close to the wavenumber ω_o and the limits of the integral can be changed without appreciable error so that

$$\varepsilon_{line} = \frac{R_{\omega o}^o}{\sigma T^4} \int_{\Delta\omega_o} (1 - e^{-SXb(\omega)}) \, d\omega \tag{4.12}$$

For a single line we define (17)

$$W_{S\ell} = \int_{\Delta\omega_o} (1 - e^{-SXb(\omega)}) \, d\omega \qquad (4.13)$$

as the equivalent line width. This concept is a very useful one and it can be shown that band emissivities are functions of $W_{S\ell}$ and spectral line separation.

In a similar way we can show that for a band, the total (engineering) emissivity is given by (1)

$$\varepsilon_{band} = \frac{\overline{R^o_{\omega_b}}}{\sigma T^4} \int_{\Delta\omega \text{ band}} (1 - e^{-P_\omega X}) d\omega$$

The values of $W_{S\ell}$, etc. are well-known for the types of line given by (4.7) and (4.8) and also for a mixture of the two. However, the calculation of the spectral band emissivity is a mammoth task and the varied assumptions that can be made manifest themselves in the results.

Provided there are a large number of lines in the band we do not concern ourselves with the high resolution calculation of spectral emissivity. The individual line shape of each spectral line is expected to be the same.

From the work of Plass (17) the two basic (and combination) models of a spectral band, and their associated approximations, will be presented briefly.

4 (b) The Equivalent Widths of Spectral Lines for Various Line Shape Parameters (17)

Directly from the definition of equivalent width we can substitute the normalized line shape parameters $b(\omega)$ and evaluate the integral. Mathematically we extend the limits of integration to infinity.

i. For a Lorentz broadened line we find

$$W_{S\ell} = 2\pi\alpha_L \, f(x) \qquad (4.14)$$

where $x = \frac{SX}{2\pi\alpha_L}$, $f(x) = x\, e^{-x}\left[I_o(x) + I_1(x) \right]$ is the Ladenburg-Reiche function, (18,26) and $I_o(x)$, $I_1(x)$ are Bessel functions of imaginary

argument. Since $x \propto \frac{1}{\alpha_L}$ for fixed SX, x is a measure of the spread of the line. There are two well-known approximations,

(a) For small x the above expression becomes

$$W_{S\ell} = 2\pi\alpha_L x = SX \qquad (4.15)$$

where $x \leq 0.02q$ for the approximation to be valid to q per cent.

This is called the weak line (or linear) approximation (W.L.A.).

(b) For large x, we find

$$W_{S\ell} = 2\alpha_L (2\pi x)^{\frac{1}{2}} \qquad (4.16)$$

where $x \gg 12.5/q$ to q per cent.

This is the strong line (or square root) approximation (S.L.A.), in which the spectral line is concentrated very close to the transition wavenumber ω_o.

The Ladenburg-Reiche (3) plot and the two approximations are shown in Fig. 7.

2. For the Doppler line shape, the integral can only be evaluated by first making the approximations. The results are then

(a) Weak line approximation

$$W_{S\ell} = SX \sum_{n=0}^{\infty} \frac{(-1)^n x_D^n}{(n+1)!(n+1)^{\frac{1}{2}}} \qquad (4.17)$$

where $x_D = \sqrt{\frac{\ell n 2}{\pi}} \frac{SX}{\alpha_D}$, and α_D is the Doppler half-width.

This series is convergent for $x_D < 1$ and also valid to q per cent when only the first term is used if $x_D < 0.03q$, in which case

$$W_{S\ell} = SX.$$

(b) Strong line approximation

$$W_{S\ell} = 2\alpha_D \sqrt{\frac{\ell n x_D}{\ell n 2}} \left[1 + \frac{c}{2} \ell n x_D \ldots \right] \qquad (4.18)$$

which varies very slowly with x_D, c being a constant of order $\frac{1}{2}$.

3. Since the square line-shape is often used as an approximation to

simplify the analysis, it is interesting to calculate its equivalent width.

In this case

$$b(\omega) = \begin{cases} 1/\delta & \text{for } (\omega_o - \tfrac{1}{2}\delta) < \omega < (\omega_o + \tfrac{1}{2}\delta), \\ 0 & \text{for } (\omega_o - \tfrac{1}{2}\delta) > \omega;\ \omega > (\omega_o + \tfrac{1}{2}\delta). \end{cases}$$

Then

$$W_{S\ell} = \int_{\omega_o - \frac{1}{2}\delta}^{\omega_o + \frac{1}{2}\delta} (1 - e^{-\frac{XS}{\delta}}) d\omega$$

$$= \delta(1 - e^{-\frac{XS}{\delta}})$$

$$= SX, \text{ for small } x_S \left(= \frac{XS}{\delta}\right)$$

It can be seen that the weak-line approximation is independent of line shape. For large values of x and mixtures of Lorentz and Doppler broadening we find that a good approximation is (19)

$$W_{S\ell} = 2\pi\alpha_L \left(\frac{2x}{\pi}\right)^{\frac{1}{2}} \left\{1 - \left(1 - \frac{3}{2a^2}\right) \frac{1}{8x} + \ldots\right\}$$

where $a = \frac{\alpha_L}{\alpha_D}(\ell n\ 2)^{\frac{1}{2}}$.

From this it is seen that even if α_D is considerably larger than α_L, the square root approximation is still valid provided x is large enough. The physical reason for this is that at large x the emissivity at the line centre becomes unity, so that the variations in absorption come mainly from the wings of the line, which are much more effective in the case of a Lorentz broadened line. (See Fig. 6).

The physical meaning of equivalent width is given by

$$W_{S\ell} = \int_{\Delta\omega} \varepsilon_\omega\, d\omega, \qquad (4.19)$$

which is the width of a line of unit spectral emissivity with the same total emissivity as the original line.

4 (c) Models of Band Spectra and Calculation of Spectral Emissivity in terms of Equivalent Widths of Single Lines

We have seen that the total emissivity of a line is related to the equivalent width of the line. That is

$$\varepsilon_{S\ell}(T) = \frac{R^{o}_{\omega o}(T)}{\sigma T^{4}} \quad W_{S\ell}(T) \tag{4.20}$$

We can also calculate $W_{S\ell}(T)$ for any line given $S(T)$ and $b(\omega,T)$.

A natural extension of these arguments includes emission and absorption of large numbers of lines in a band. For a band made up of superposed lines we can calculate the total fractional absorption $A(T)$ which is the total hemispherical emissivity of the band, under the conditions of Kirchhoff's Law, $\varepsilon_{band}(T) = A(T)$.

There are two basic models of an absorption band:

(1) The Elsasser Model, and

(2) The Statistical Model.

(1) The Elsasser Model (20, 19)

The Elsasser band contains an infinite number of equally spaced lines with equal intensity and identical line shape parameters.

The fractional absorption of the band is found to be represented in the form of an integral which cannot be evaluated in terms of elementary functions, but can be approximated by:

(a) $A = \mathrm{erf}(\frac{1}{2}\beta^{2}x)$; Valid if $x>1.25$, $\beta<0.3$ (to 10 per cent),

(b) $A = 1 - e^{-\beta x}$; valid if $\beta>3$, for all x, (to 10 per cent),

where $\beta = \frac{2\pi\alpha}{d}$, $x = \frac{SX}{2\pi\alpha} = \frac{SX}{\beta d}$, d being the line separation.

If we consider the physical interpretation of $W_{S\ell}$ given in (4.19) it is very easy to see that the fractional absorption for a Lorentz-line band is given by

$$A = \frac{W_{S\ell}}{d} = \beta \quad f(x).$$

This expression is correct to 10 percent if $x<0.06\beta^{-2}$ and $\beta<0.3$ or $x<0.2\beta^{-1}$ and $\beta>0.3$.

Note that (4.20) no longer applies since we assumed that $R^{o}_{\omega_o}$ was constant over a spectral line. Here we have many equally spaced lines and $R^{o}_{\omega_o}$ is certainly not constant across them all.

(2) The Statistical Model (17)

Whereas the Elsasser Model is one of a perfectly regular frequency spectrum, the spectral distribution of lines in the statistical model is random, as is the intensity of each line. In fact position and intensity are governed by probability distribution functions. No correlation between lines is assumed, and it can be shown that the absorption is a function only of the equivalent width of a single line of the band.

Define $N(\omega_1, \ldots \omega_n)d\omega_1 \ldots d\omega_n$ as the probability that the first line will be in the wavenumber range $d\omega_1$ at ω_1 while the second line is in the range $d\omega_2$ at ω_2, and so on up to line n. Take the wavenumber origin at the centre of a band of width D. Define also $P(S_i)dS_i$ as the probability that the intensity of the ith line is in the range dS_i at S_i. The spectral emissivity of the ith line with a shape $b(\omega_i)$ is therefore $(1 - e^{-S_i X\, b(\omega_i)})$ which is also the fractional spectral absorption for an optical path length X. The total absorption A for a statistical band is then

$$A = 1 - \frac{\int_{-\frac{1}{2}D}^{\frac{1}{2}D} \cdots \int_{-\frac{1}{2}D}^{\frac{1}{2}D} N(\omega_1 \ldots \omega_n)d\omega_1 \ldots d\omega_n \int_o^\infty \cdots \int_o^\infty \prod_i P(S_i)e^{-XS_i b(\omega_i)} dS_i}{\int_{-\frac{1}{2}D}^{\frac{1}{2}D} \cdots \int_{-\frac{1}{2}D}^{\frac{1}{2}D} N(\omega_1 \ldots \omega_n)d\omega_1 \ldots d\omega_n \int_o^\infty \cdots \int_o^\infty \prod_i P(S_i)dS_i} \qquad (4.21)$$

Since no correlation between the frequencies $\omega_1, \ldots \omega_n$ is assumed, N must be a constant, and if we normalize $P(S_i)$ so that

$$\int_o^\infty P(S_i)dS_i = 1,$$

then since the intensities are unrelated the integral over each line is equal to the integral over any other line, and A reduces to

$$1 - \left\{\frac{1}{D} \int_{-\frac{1}{2}D}^{\frac{1}{2}D} d\omega \int_o^\infty P(S)e^{-SXb(\omega)} dS \right\}^n$$

By further mathematical rearrangement we find that

$$A = 1 - \left\{1 - \frac{1}{D} \int_{-\frac{1}{2}D}^{\frac{1}{2}D} d\omega \int_{o}^{\infty} P(S)\ (1 - e^{-SXb(\omega)})dS \right\}^n$$

$$= 1 - \left\{1 - \frac{1}{D} \int_{o}^{\infty} P(S)dS \int_{-\frac{1}{2}D}^{\frac{1}{2}D} (1 - e^{-SXb(\omega)})\ d\omega\right\}^n$$

$$= 1 - \left\{1 - \frac{1}{D} \int_{o}^{\infty} P(S)\ W_{S\ell,D}(S,\alpha)dS\right\}^n$$

$$= 1 - \left\{1 - \frac{1}{D}\ \overline{W_{S\ell,D}(\overline{S},\alpha)}\right\}^n \qquad (4.22)$$

where $\overline{W_{S\ell,D}(\overline{S},\alpha)}$ is the mean value of $W_{S\ell,D}(S,\alpha)$ over the distribution P(S) in the bandwidth D. $\overline{S}$ is some standard intensity within P(S).

Now D = nd, where d is the average line spacing in the band, so that

$$A = 1 - \left\{1 - \frac{\overline{W_{S\ell,D}(\overline{S},\alpha)}}{nd}\right\}^n ,$$

If the number of lines n, approaches infinity while d remains constant, that is $D \to \infty$, then

$$A = 1 - e^{-\frac{\overline{W_{S\ell}(\overline{S},\alpha)}}{d}} , \qquad (4.23)$$

where $$W_{S\ell}(S,\alpha) = \int_{o}^{\infty} (1 - e^{-SXb(\omega)})d\omega,$$

and $$\overline{W_{S\ell}(\overline{S},\alpha)} = \int_{o}^{\infty} P(S)\ W_{S\ell}(S,\alpha)dS. \qquad (4.24)$$

These results demonstrate that for any value of n, the fractional

absorption of a band, including all overlapping effects, can be represented as a function of the equivalent width of the spectral line.

It can be shown that provided the number of lines in the band exceeds ten, the predicted absorption curves (a plot of A vs. x for fixedβ, where x and β refer to a single line in the band) are almost identical (see Fig. 8) for all values of absorption of practical interest. ($0.01<A<1$).

It can also be shown that the fractional absorption is nearly independent of the function P(S).

For a square line,

(i) For $P(S) = \delta(S - \overline{S})$, i.e. equally intense lines.

$$\overline{W_{S\ell}} = \delta\left(1 - e^{-\frac{X\overline{S}}{\delta}}\right)$$

(ii) For $P(S) = \frac{1}{\overline{S}} e^{-S/\overline{S}}$, i. e. an exponential intensity distribution.

$$\overline{W_{S\ell}} = \frac{X\overline{S}}{1 + \frac{X\overline{S}}{\delta}}$$

These two expressions for $\overline{W_{S\ell}}$ are very similar, especially if $\frac{X\overline{S}}{\delta} \ll 1$, which is the W.L.A.. In fact, providing we correlate all the values of $\overline{S}$ for the various intensity probability functions, we can get nearly complete agreement for any reasonable intensity probability function $P(S,\overline{S})$. (17)

Note that in the W.L.A.:-

$$\overline{W_{S\ell}(\overline{S},\alpha)} = \int_0^\infty SX\, P(S)dS = X\overline{S} .$$

A comparison between models (1) and (2) is shown in the plot of fractional absorption curves in Fig. 9.

Since, on the whole, molecular spectra are neither a completely random nor perfectly regular set of lines, the obvious generalization of the above two models is the Random Elsasser Model (17). This is a random superposition of pure Elsasser bands of varying total intensity and line spacing. The result of an argument similar to that given for pure statistical model leads us to

$$A = 1 - \left[\prod_{i=1}^{N} (\Delta_i) \right]^{-1} \int_{-\frac{1}{2}\Delta_1}^{\frac{1}{2}\Delta_1} \cdots \int_{-\frac{1}{2}\Delta_N}^{\frac{1}{2}\Delta_N} d\omega_1 \cdots d\omega_N \int_0^\infty \cdots \int_0^\infty \prod_{i=1}^{N} P_E(S_i) e^{-SiXb_i(\omega_i)} dS_i, \qquad (4.25)$$

where Δ_i denotes the line separation of the ith Elsasser band of which there are N; $b_i(\omega_i)$ being the line shape factor summed over all the lines of the ith band ; $P_E(S_i)d S_i$ is the probability that the ith Elsasser band has total intensity in the range dS_i at S_i.

The expression reduces to

$$A = 1 - \prod_{i=1}^{N} \left(1 - \frac{\overline{W_{E,i}}}{\Delta_i}\right). \qquad (4.25)$$

Here, $\overline{W_{E,i}} = \int_0^\infty W_{E,i}(x_i, \beta_i)\, P(S_i) dS_i$, with $\beta_i = \frac{2\pi\alpha_i}{\Delta_i}$

and $x_i = \frac{SiX}{2\pi\alpha_i}$;

$$\overline{W_{E,i}} = \int_0^\infty \Delta_i A_{E,i}(x_i, \beta_i)\, P(S_i) dS_i,$$

where $A_{E,i}(x_i, \beta_i)$ is the absorption due to the ith band.

This formulation of the Random Elsasser band allows us to find an infinite set of absorption curves (i.e. A vs. x for fixed β), between those given by the statistical model and the Elsasser Model, depending on the number and intensity of Elsasser bands we consider, (see Fig. 10).

Further, as $N \to \infty$ and the average line spacing d, given by

$$\frac{1}{d} = \sum_{i=1}^{N} \frac{1}{\Delta_i},$$

is held constant, the absorption curve approaches that of the statistical model. For example if S_i , α_i and Δ_i are independent of i,

$$\overline{W_{E,i}\ (x_i,\ \beta_i)} \quad = \quad \overline{W_L(x,\beta)}$$

so that $A = 1 - (1 - \frac{\overline{W_E}}{Nd})^N$

$$= 1 - e^{-\frac{\overline{W_E}}{d}} \quad \text{as } N \to \infty \ ;$$

which is a statistical model result.

In most molecular bands at high temperatures this number of superposed bands is so large that the statistical model has been used in emissivity calculations, (particularly for carbon dioxide).

5. Application of the Statistical Model to the Vibration-Rotation Bands of Diatomic and Linear Triatomic Molecules, taking the 4.3 micron Carbon Dioxide Band as an Example in Calculating the Spectral Emissivity.

We have seen in Section 2 that the relative intensity of single spectral lines in a vibration-rotation band can be calculated as a function of the rotational quantum number. In Section 3 (b) we saw that the integrated band intensity can be found at any temperature if its value at one temperature is known.

This information allows us to calculate the spectral emissivity of a vibration-rotation band but would involve consideration of each individual line of the band and there may be well over 100,000 of these at high temperatures. There is however a 'reverse' method formulated by Malkmus and Thomson (21) for diatomic molecules and adapted by Malkmus (13) for the 4.3 micron band of carbon dioxide.

This method assumes a diatomic molecular model consisting of an anharmonic vibrator and rotator with the first order vibration-rotation interaction.

The energy states of this model can be expressed in terms of vibrational and rotational quantum numbers. The transition wavenumber from state (n,j) to state ((n+1), j') is given by

$$\omega = \omega(n) + B_e\Big[\ j'(j'+1) - j(j+1)\Big] \ - \alpha_e \Big[(n + {}^3/_2)(j'+1)j' - (n+\tfrac{1}{2})j(j+1)\Big],$$

(5.1)

where $\omega(n)$ is the central wavenumber of the band and depends only on vibrational quantum number n, and potential well constants. B_e is the rigid rotator spectroscopic constant and α_e is the first order vibration-rotation interaction constant.

The rotational selection rule informs us that

$$j' = j \pm 1 \qquad (\text{with } j,\ j' \geq 0),$$

leading us to two expressions for ω, one for each branch of the band. There is no Q-branch for a diatomic molecule, and for a parallel band of a linear triatomic molecule the Q-branch is very weak. The P- and R-branches have lines at the following spectral positions:

$$\omega = \omega(n) + B_e \begin{Bmatrix} 2(j+1) \\ -2j \end{Bmatrix} - \alpha_e \begin{Bmatrix} j(j+1) - 2(j+1)(n+3/2) \\ j(j+1) - 2j(n+3/2) \end{Bmatrix} \qquad (5.2)$$

The upper expression corresponds to $j' = j + 1$ (R-branch) and the lower expression to $j' = j - 1$ (P-branch). By substituting $j = m - 1$ into the upper expression and $j = -m$ into the lower one two identical expressions are derived:

$$\omega = \omega(n) + 2m B_e - \alpha_e \left[m(m+1) + 2m(n+\tfrac{1}{2}) \right] \qquad (5.3)$$

This single expression describes both the R- and P- branches by means of the appropriate substitution for m. Equation (5.3) is then solved as a quadratic equation in m leading to two solutions

$$m_1 = \frac{B_e - \alpha_e(n+1) - \sqrt{(B_e - \alpha_e(n+1))^2 - \alpha_e(\omega - \omega(n))}}{\alpha_e}$$

and

$$m_2 = \frac{B_e - \alpha_e(n+1) + \sqrt{(B_e - \alpha_e(n+1))^2 - \alpha_e(\omega - \omega(n))}}{\alpha_e}$$

which Malkmus and Thomson associated with the P- and R-branches respectively.

The expression for the integrated line intensity of a single line in each branch of the band can be found absolutely as a function of the vibrational and rotational quantum numbers of the initial state (n, j) and

spectroscopic constants (31). By substituting $j = j(m)$ we can find the integrated line intensity for the band as a function of m. Further by substituting $m_1 = m_1(\omega)$ and $m_2 = m_2(\omega)$ above we can find the integrated line intensity as a function of (n, ω). This operation involves a smoothing out of quantum numbers, but since there are many lines this does not cause any trouble if only low resolution spectroscopy is required. Application of the Statistical Model of a band enables us to complete the low resolution spectral emissivity of the band.

Thus from $S = S(n \to n', j \to j')$ we can find

$$S = S(n \to (n+1), \omega)$$

and hence the spectral emissivity. For example in the weak line approximation, we find, from Equ (4.23), that

$$\varepsilon_\omega = 1 - \exp\left(-\frac{p\,\bar{S}(\omega)}{d(\omega)}\right)$$

where now we have

$$\frac{\bar{S}(\omega)}{d(\omega)} = \sum_{n=0}^{\infty} \left\{ \left(\frac{S_n^{n+1}(\omega)}{d_n(\omega)}\right)_{m_1} + \left(\frac{S_n^{n+1}(\omega)}{d_n(\omega)}\right)_{m_2} \right\} \qquad (5.4)$$

Here $d_n(\omega)$ is the mean line separation in the band and is given by

$$d_n(\omega) = 2\sqrt{\left[B_e - \alpha_e(n+1)\right]^2 - \alpha_e(\omega - \omega(n))}\ . \qquad (5.5)$$

For computation of ε_ω by this method physical conditions of pressure, temperature, and optical path length are chosen, and for a given wavenumber $(S(\omega)/d(\omega))$ can be calculated using the summation.

Malkmus and Thomson (21, 13) associated the two solutions of the quadratic equation (5.3), that is m_1 and m_2, with the P- and R-branches of the spectral band. In fact the solution m_1 describes both the P- and R-branches up to the band head in the R-branch. The solution m_2 describes only that part of the band beyond the band head. In this region the rotation-vibration interaction energy in the first-order approximation is larger than the rotational energy, and higher order interaction terms should be considered. Fig. 33, which shows a plot of equation (5.3), should help to clarify this point.

It happens that the intensity of the spectral lines approaches zero rapidly beyond the band head, so that the contribution to the emissivity of the spectral lines described by m_2 is very small. The error in the emissivity, caused by neglecting the solution m_2, is very much less than the main errors of the calculation. These stem from the use of the harmonic oscillator approximation in predicting the spectral line intensities and the use of an approximate spectral band model.

Thus, to within the accuracy of the models used in the calculation we can neglect the term

$$\left(\frac{S_n^{n+1}(\omega)}{d_n(\omega)} \right)_{m_2}$$

in equation (5.4).

We can now proceed with a summary of the work done by Malkmus (13) on the 4.3 micron band of carbon dioxide.

The similarity of the 4.3 micron band of carbon dioxide to that of a diatomic molecule has been noted in section 2(b). The 4.3 micron band consists of two types of superposed bands.

(i) Those for which $\ell=0$, when alternate lines (of odd j) are absent, but the remaining lines have twice the intensity expected from diatomic theory

(ii) Those for which $\ell>0$, when the average line intensity is the same as for diatomic molecules, but there are twice as many lines in the band, (see Fig. 1). A weak central branch is also formed, becoming stronger as ℓ increases, but since the lines near the band centre become weaker as ℓ increases, both effects are ignored. Even at 3000°K the average value of ℓ is only about three.

The spectral emissivity is calculated for both the W.L.A. and S.L.A. and also for Lorentz and Döppler lineshapes.

In the weak line approximation we saw that $W_{S\ell} = SX$; leading to $\overline{W}_{S\ell} = \overline{SX}$, and now with the arguments laid out as above $\overline{S}$ can be regarded as a function of wavenumber. Thus

$$\varepsilon_\omega = A_\omega = 1 - e^{-\frac{\overline{S}(\omega)p1}{d(\omega)}} \qquad (5.6)$$

Using the methods of Section 3(b) we can eliminate the quantum numbers ℓ, n_1 and n_2 and replace them by a combined quantum number n and a degeneracy factor.

The corrected equation (5.4) becomes

$$\frac{\overline{S}(\omega)}{d(\omega)} = \sum_{n=0}^{\infty} \sum_{n_3=0}^{\infty} \left(\frac{S_{nn3}(\omega)}{d_{nn3}(\omega)} \right) \qquad (5.7)$$

where $S_{nn_3}(\omega) = \dfrac{\alpha_{nn_3} B_e hc\omega}{\omega_{nn_3} kT} (1 - e^{-\frac{hc\omega}{kT}})(1 - e^{-\frac{hc\omega_{nn_3}}{kT}})^{-1}$

$$\times \left| \frac{L - \sqrt{L^2 - K}}{\alpha_3} \right|$$

$$\times \exp\left\{ -\frac{hcL}{k\alpha_3 T} \left[2L(L^2 - \sqrt{L^2 - K'}) - \left(1 + \frac{\alpha_3}{2L} \right) . K \right] \right\} \qquad (5.8)$$

and $d_{nn_3}(\omega) = 2\sqrt{L^2 - K}$, (5.9)

where $L = B_e - \alpha_1(n_1 + \frac{1}{2}) - \alpha_2(n_2 + 1) - \alpha_3(n_3 + 1)$, (5.10)

and $K = \alpha_3(\omega - \omega_{nn_3})$. (5.11)

ω_{nn_3} and α_{nn_3} are defined in Equs. (3.5) and (3.16).

The constants B_e, α_1, α_2, α_3 are given in earlier papers (for example see Ref. 22). Since $\alpha_1 \approx -2\alpha_2 << B_e$, Malkmus neglected contributions due to α_1 and α_2. Here we have considered only one root of the quadratic equation (5.2) when the approximation to the vibration rotation interaction is most valid.

In the S.L.A. for Lorentz-type lines we saw

$$W_{S\ell} = 2\alpha_L(2\pi x)^{\frac{1}{2}} = 2(\alpha_L S X)^{\frac{1}{2}},$$

and it is necessary that (a) lines grouped together are not considered exactly superposed, (b) the $\ell = 0$ bands have a spacing and intensity different from the other bands. Since $\alpha_L = \alpha_L(p,T) \propto p$, we put $\alpha_L = \alpha_o p$, p being the pressure in atmospheres.

Thus, $W_{S\ell} = 2\alpha_o^{\frac{1}{2}} p^{\frac{1}{2}} S^{\frac{1}{2}} (pl)^{\frac{1}{2}}$

$= 2\alpha_o^{\frac{1}{2}} S^{\frac{1}{2}} (p^2 l)^{\frac{1}{2}}$.

Therefore $\epsilon_\omega = 1 - \exp\{-2\alpha_o^{\frac{1}{2}} (p^2 l)^{\frac{1}{2}} \frac{\overline{S}^{\frac{1}{2}}(\omega)}{d(\omega)}\}$ (5.12)

where $\frac{\bar{S}^{\frac{1}{2}}(\omega)}{d(\omega)} = \sum_{n=0}^{\infty} \sum_{n_3=0}^{\infty} (\tfrac{1}{2}\rho^n)^{\frac{1}{2}} \frac{(S_{nn_3}(\omega))^{\frac{1}{2}}}{d_{nn3}(\omega)}$

where ρ^n is given by (3.14). For a mixture of gases with a total pressure P_T and CO_2 partial pressure of P_p, in the weak line approximation $(p1)$ becomes $(p_p 1)$, and in the strong line approximation $(p^2 1)^{\frac{1}{2}}$ becomes $(p_T p_p 1)^{\frac{1}{2}}$.

For Doppler line shape we had

$$W_{S\ell} = SX \sum_{m=0}^{\infty} \frac{(-1)^m x_D^m}{(m+1)!(m+1)^{\frac{1}{2}}} , \qquad (5.14)$$

where $x_D = \sqrt{\frac{\ell n 2}{\Pi}} \times \frac{SX}{\alpha_D}$.

Assuming the statistical model we find

$$= 1 - \exp\left[- \sum_{n=0}^{\infty} \sum_{n_3=0}^{\infty} \frac{W^{*S\ell}_{nn_3}}{d_{nn_3}} \right] \qquad (5.15)$$

where $W^{*S\ell}_{nn_3} = S^*_{nn_3} \cdot X \cdot \sum_{m=0}^{\infty} \frac{(-1)^m \left[\frac{S^*_{nn_3}(\omega)}{\alpha_D} \sqrt{\frac{\ell n 2}{\Pi}} \right]^m}{d^*_{nn3}}$ (5.16)

$$S^*_{nn3}(\omega) = \frac{2}{\rho^n} \cdot S_{nn_3}(\omega) ,$$

and $d^*_{nn_3} = \frac{2}{\rho^n} \cdot d_{nn_3}(\omega)$, which were given previously.

Wallmus calculated the emissivities in both W.L.A. and S.L.A. for T = 300°K, 600°K, 1200°K, 1800°K, 2400°K, 3000°K. For purpose of calculating $\alpha_{oo}(T)$ he assumed that the total band strength (23) at 300°K

was 2700 cm.$^{-2}$ atm.$^{-1}$. That is

$$\sum_{n=0}^{\infty} \sum_{n_3=0}^{\infty} \alpha_{nn_3}(300^{o}) = 2700 \text{ cm.}^{-2} \text{ atm.}^{-1}$$

Since $\frac{\alpha_{nn_3}(T)}{\alpha_{oo}(T_o)}$ is known, $\alpha_{nn_3}(T_o)$, and $\alpha_{nn_3}(T)$ can be found.

The value of $\alpha_o(24)$ was assumed to be 0.064 cm^{-1} at 300^{o}K and to vary as $T^{-\frac{1}{2}}$. The accuracy of this value is questionable as it is based on measurements of the nitrogen-broadened 15μ band. The values of nn_3 considered were limited by taking into account only those states for which the fractional population $N^{nn3}(T)$ was greater than 10^{-3} of the maximum value of $N^{nn3}(T)$. Since the intensity of each "average spectral line" was calculated it would have been just as easy to leave out all those lines weaker than a given strength, rather than leaving out all states with less than a given fractional population, especially as line strength is a function of dipole moment as well as level population. Also the presence of 1.1 per cent of $C^{13}O^{16}_2$ was ignored. The error here would be more noticeable at lower temperatures.

Use of the above formulae enables us to compute the exponents involved in the expressions for the emissivity.

Figs. 11 to 16 show the variation of $\overline{S}/_d$ and $2\alpha_o{}^{\frac{1}{2}}\overline{S}^{\frac{1}{2}}/_d$ with wavenumber for the temperature already specified and also the variations with temperature of $\overline{S}/_d$ for wavenumbers ω in the range

$$1900 \leq \omega \leq 2390 \text{ cm.}^{-1}$$

Figs. 17 to 20 show the emissivity curves for weak line approximation and Doppler line shape for the temperatures 300; 600; 1200; 1500^{o}K. It is seen that the pure Doppler line shape provides a lower limit to ε_ω, for any given conditions. The agreement between W.L.A. and pure Doppler emissivities is seen to improve with increasing temperature and decreasing optical path length.

Figs. 21 and 22 compare the W.L.A. with that derived by Plass (27) for T = 1200^{o}K and 2400^{o}K. The discrepancies are alarming, particularly at the higher temperature, when the two curves are separated by a factor of about 15 for any given wavenumber, but the general shape is seen to agree fairly well. However Plass's results have been shown to be inconsistent with the harmonic approximation in completing the integrated band intensities, (28). The same tendencies are found by comparing the S.L.A. in both Plass's and Malkmus's work (13).

Figs. 23 to 25 compare the emissivity with Ferriso's experimental (supersonic burner) results (28). The W.L.A. is seen to improve with temperature. This we expect since the number of lines increases rapidly with temperature. Fig. 23 shows also the S.L.A. computation of ε_ω, which is

seen also to predict a value larger than the observed one. In fact in the absence of Doppler broadening each of these approximations separately provide an upper limit to ε_ω. When the spectrum is one of a few strong lines superposed on a background of many weak lines, neither W.L.A. or S.L.A. is a good approximation. In this case the value of the summand in the two cases is computed separately for each superimposed band, and the lower of the two values is taken. i.e. we take the smaller of the two terms:

$$p\ell \frac{S_{nn3}(\omega)}{d_{nn3}(\omega)} \quad , \text{ and}$$

$$2\alpha_o^{\frac{1}{2}}(p^2\ell)^{\frac{1}{2}}(\tfrac{1}{2}\pi)^{\frac{1}{2}} \qquad \frac{S_{nn3}(\omega)^{\frac{1}{2}}}{d_{nn3}(\omega)} \quad .$$

Since the error in both terms is known to be such that both terms are too large we shall get a better result by always taking the smaller one. The procedure is not purely empirical, but assigns the most valid approximation to each band and of course gives a more accurate result than either W.L.A. or S.L.A. alone, as can be seen in Figs. 23, 26, 27 and 28, where the shape of the curve is reasonably well predicted. The asymetric peak in the experimental curve of Ferriso at 2400°K may be due to over-correction for atmospheric absorption.

Figs. 26 and 27 compare the results with those of Tourin's gas-cell observations (14) at 1200°K. The two figures are different only in that the carbon dioxide is pressurized in Fig. 27 by 0.855 atm. of nitrogen. The W.L.A. yields the same curve for ε_ω whereas the other approximations are better in the case of pure CO_2. Thus the nitrogen does not broaden the individual lines of the band as much as our models. As the value of α_o at 300°K is questionable this is one of the possible sources of error.

Fig. 28 shows similar comparisons at a different optical path length to Burch's results (29) at 1200°K, and Figs. 29 and 30 compare these results in the strong and weak line approximations to those of Oppenheim and Ben-Aryah (25), who use the statistical model to calculate transmittance (Section 6).

It is worth noting that in the strong line approximation, where

$$\varepsilon_\omega = 1 - e^{-2\alpha_o^{\frac{1}{2}}\bar{S}^{\frac{1}{2}}(p^2\ell)^{\frac{1}{2}}/d} \quad ;$$

the emissivity is not a function of $X = p\ell$, so that the elementary law of absorption (Lambert-Beer's Law) is not obeyed. The Lambert-Beer's Law expresses $\varepsilon_\omega = \varepsilon_\omega(p\ell)$ in the form

$$\varepsilon_\omega = 1 - e^{-k_\omega p\ell}$$

where k_ω is the spectral absorption coefficient.

Thus a consequence of the S.L.A. is loss of linearity in optical path length.

It is evident that the mixed weak-strong line approximation is more accurate than either W.L.A. or S.L.A. alone, though the estimate of emissivity is still too large. However pure Doppler line shape always under-estimates ε_ω. So that we can at least calculate the two limits between which the true emissivity curve lies.

6. Direct Application of the Statistical Model at 1200°K, in order to Verify its Validity, and to Derive an Expression for the Spectral Absorption (25)

Consideration of quantum jumps and individual spectral lines is laid aside and the statistical model, as described in Section 4, is used to attempt to find from some simple absorption experiments the empirical laws governing the band radiation. The study is confined to Lorentz lines only, for which the full Ladenburg-Reiche function is used to replace its asymptotic limits of the Weak and Strong Line Approximations for the equivalent width.

The situation considered is a cell of gas of length 'ℓ' at a constant temperature of 1200°K. The experimental variables are the pressure p and ℓ. Only pressures greater than 0.071 atms. were used in the experiments, since below this, at 1200°K, Doppler broadening has a significant effect.

The statistical model was given in Section 4, where we had the result that the fractional absorption A could be represented by the expression (19)

$$A = 1 - \exp - \frac{\overline{W}_{S\ell}}{d} \qquad (6.1)$$

Where

$$\overline{W_{S\ell}}\ (\overline{S},\ \alpha,\ p,\ \ell) = \int_0^\infty W_{S\ell}(S,\ \alpha,\ p\ell\ )\ P(S,\ \overline{S})\ dS,$$

$P(S, \overline{S})$ being the intensity probability function and $\overline{S}$ some mean intensity. Since the dependence of A on the actual form of $P(S, \overline{S})$ is small (17), we shall use throughout the distribution

$$P(S,\overline{S}) = \delta(S - \overline{S}),$$

where δ is the Dirac δ-function.

Also in (6.1), d is the mean line spacing in the band. Since there

are many lines in the band, across which we consider the Planck radiation function to be constant, we shall consider that A, $W_{S\ell}(\alpha, S)$ and α are functions of wavenumber denoted by A_ω, $W_{S\ell,\omega}(\alpha_\omega, S_\omega)$ and d_ω.

Now, since we are studying pure Lorentz lines for which the half-width is proportional to pressure, that is

$$\alpha_\omega = \alpha^o_\omega p,$$

it follows that $W_{S\ell,\omega} = W^o_{S\ell,\omega} p$, where the superfix ^{o} denotes all quantities at unit pressure. Also, by definition

$$S_\omega = S^o_\omega p .$$

Assuming the Dirac intensity probability function, it follows that

$$A_\omega = 1 - e^{-\frac{W^o_{S\ell,\omega}}{d_\omega} p} \tag{6.2}$$

For pure Lorentz lines $W^o_{S\ell,\omega} = 2\pi\alpha^o_\omega f(x_\omega)$, where $x_\omega = \frac{S^o_\omega \ell}{2\pi\alpha^o_\omega} = \frac{S_\omega \ell}{2\pi\alpha_\omega}$

for this special case of $p = 1$, and $f(x_\omega)$ is the Ladenburg-Reiche function, shown in Fig. 7, and given by

$$f(x_\omega) = x_\omega e^{-x_\omega} \left[I_o(x_\omega) + I_1(x_\omega) \right] .$$

Therefore, for purposes of calculating $W^o_{S\ell,\omega}$, x_ω is independent of pressure.

Denoting the spectral transmission by T_ω it follows from (6.2) that

$$\begin{aligned} -\ell n\, T_\omega &= -\ell n\, (1 - A_\omega) \\ &= p \frac{W^o_{S\omega,}}{d_\omega} , \end{aligned}$$

since

$$\overline{W^o_{S\ell,\omega}} = W^o_{S\ell,\omega},$$

and a plot of $-\ell n T_\omega$ versus p results in a straight line through the origin.

However this does not constitute a proof of the statistical model since the simple Lambert-Beer's Law also states that

$$-\ell n\ T_\omega = p\ k_\omega \ell\ ,$$

leading to a linear plot.

Comparison of the above two absorption laws shows that we should also consider ℓ as a variable, since it is implied that $\frac{W^o_{S\ell,\omega}}{d_\omega}$ is a function of ℓ if the laws are to agree over some range of (p,ℓ). In fact this dependence on ℓ is quite pronounced and is represented in the Ladenburg-Reiche curve.

Thus since

$$T_\omega = \exp\ \{-(\frac{2\pi\alpha^o_\omega}{d_\omega})\ p\ \ f\ (x_\omega)\ \} \qquad (6.3)$$

a plot of $-\frac{\ell nT_\omega}{p}$ versus ℓ for a fixed frequency should follow the Ladenburg-Reiche curve. Once this plot is shown to agree with the theoretical curve we have proved the validity of the statistical model.

The function $W^o_{S\ell,\omega}$ is mathematically determined by the parameters S^o_ω and α^o_ω, integrated intensity and half-width at unit pressure. Thus A_ω is fully determined by $(\frac{S^o_\omega}{d_\omega})$ and $(\frac{\alpha^o_\omega}{d_\omega})$ which may be read off from the Ladenburg-Reiche curve, once constructed.

The following procedure is useful

(i) A recording of the absorption spectrum of the band, measured from a cell of fixed ℓ and arbitrary pressure, for the pure gas is made.

(ii) Equation (6.2) allows a calculation of $(\frac{W^o_{S\ell,\omega}}{d_\omega})$ for many values of ω.

(iii) (i) and (ii) are repeated for a number of cell lengths, and for each wavenumber the values of $\frac{W^o_{S\ell,\omega}}{d_\omega}$ are plotted against ℓ on a log-log scale, that is a graph of

$$\frac{2\pi\alpha^o_\omega}{d_\omega}\quad f(x_\omega)\quad \text{vs.}\quad \ell(=\frac{2\pi\alpha^o_\omega}{S^o_\omega}\ x_\omega)\quad \text{for fixed } \omega.$$

(iv) Fitting these curves to that of

$$f(x_\omega) \quad \text{vs.} \quad x_\omega ,$$

values of $(\frac{x}{\ell})_\omega$, $(\frac{S^o}{\alpha^o})_\omega$, $(\frac{\alpha^o}{d})_\omega$ and $(\frac{S^o}{d})_\omega$ can be found.

(v) These quantities, experimentally established, give us a value of A_ω for any value of pressure or geometric path length since

$$A_\omega = 1 - \exp\{-2\pi(\frac{\alpha^o}{d})_\omega \; p \; f(\frac{\ell}{2\pi}(\frac{S^o}{\alpha^o})_\omega)\} \tag{6.4}$$

The values of $(\frac{x}{\ell})_\omega$ and $(\frac{\alpha^o}{d})_\omega$ can be used to predict the effects of gas mixtures, provided that α^o_ω is corrected to include foreign-gas broadening effects. For example, if we assume that the half-widths due to self and foreign-gas broadening are equal we find

$$x_\omega = \frac{S^o_\omega \ell}{2\pi\alpha^o_\omega} \; \frac{p}{p_T}$$

where p_T is the total pressure, and if in a series of experiments ℓ is constant and p/p_T is constant, it follows that $W^o_{S\ell,\omega}$ is unchanged, since

$$A_\omega = 1 - e^{-(\frac{W_{S\ell,\omega}}{d})_\omega \; p_T} \tag{6.2a}$$

The gas-cell experiments were performed by Oppenheim and Ben-Aryah for five different cell-lengths (25). The results are plotted on the Ladenburg-Reiche curve (18) in Fig. 31, showing good agreement at $\omega = 2273$ cm^{-1}. Thus the statistical model is a good approximation to the 4.3 micron band at 1900°K and the dependence on (p, ℓ) is also predicted. This elevated temperature was of course used to increase the number of lines in the band, making the statistical model a more feasible approximation.

In the experiment it was necessary to record a smoothed absorption curve, since it is the overall band shape that is important, and not local peaks due to a large spectral line. Thus the slitwidth of the spectrometer was increased until a reasonably smooth curve was observed. This slitwidth was 2 to 3 cm^{-1} and the bandwidth investigated was 2200 to 2400 cm^{-1}. In this sense T_ω is an average over a bandwidth of 2 to 3 cm^{-1}.

The full results are shown in the form of graphs in the original paper. The curves shown in Fig. 32 are the results of the computations outlined above where the curves have been replotted for more suitable path lengths. These curves may be used to predict the absorption in experiments using gas mixtures in the following way:

(i) For a given path length ℓ' select a figure for which $\ell \leq \ell'$, where ℓ is the path length in the figure.

(ii) Select an experimentally convenient pressure p from the figure.

(iii) For a gas mixture for which the total pressure $p_T = p$ and the partial pressure is p', such that $p' = p\ (\frac{\ell}{\ell'})$, the transmittence is given by the curve selected in (i), (ii).

This procedure neglects foreign-gas broadening effects.

Most workers, prior to Oppenheim and Ben-Arvah, (25) who measured carbon dioxide absorption for the 4.3 micron band assumed the validity of the Lambert-Beers Law, which predicts a linear dependence of $-\ell n T_\omega$ on pressure. This dependence was indeed found, but the gradients of the lines predicted very different values of the absorption coefficient, for various values of pressure and cell-length and also various methods of heating. Thus Tourin (14) (quartz gas-cell) found a value of $k_\omega = 1.09$ cm.$^{-1}$ atm.$^{-1}$ at 4.4 micron, while Steinberg and Davies (30)(Shock Tube) found $k = 2.9$ cm.$^{-1}$ atm.$^{-1}$ at the same wavenumber and conditions.

Assuming the statistical model it is possible to reconcile all these published results, using (6.2) or (6.2a) as the correct absorption Law. These results are correlated on the Ladenburg-Reiche plot (18) (Fig.31) showing that all the points fall reasonably near to the theoretical curve. This also confirms the method of accounting for the effects of foreign gases, which consists of plotting values of $-\frac{\ell n T_\omega}{p}$, for a given ℓ, partial pressure p' and total pressure p_T with an abscissa of $(\frac{p'}{p_T}\ell)$. The ordinate of each point was taken equal to $-\frac{\ell n T_\omega}{p_T}$.

Thus, given the values of two of the following:

$$(\frac{x_\omega}{\ell}),\quad (\frac{S^o_\omega}{\alpha^o_\omega}),\quad (\frac{\alpha_o}{d}_\omega)\quad \text{and}\quad (\frac{S^o}{d}_\omega),$$

which have been defined in this section, we can calculate the absorption

$$A_\omega = 1 - e^{-\frac{N S \ell, \omega}{d_\omega}},$$

as a function of temperature and wavenumber.

Of course, knowing the fractional absorption allows us to find the emissivity using Kirchhoff's Law.

8. Conclusion and a Brief Discussion of Spectral and Molecular Models

We have seen that there are two apparently quite different methods available for calculating the spectral emissivity or absorptivity of a vibration-rotation band.

The first and most important method is the fundamental one of considering individual quantum mechanical transitions, and performing summations over various degenerate states in each vibrational level.

The second method is that which is applied direct to the spectrum, ignoring all quantum mechanical transitions, and considers a model spectrum - that of the statistical model for an infinite number of lines.

Each method of attack requires some fundamental knowledge, which can only be obtained experimentally.

In the fundamental method this knowledge is in the form of spectroscopic constants concerning:

(i) energy level magnitudes and separation (22),

(ii) anharmonic potential terms (6, 7, 8),

(iii) the effects of multipolar transitions (4),

(iv) dipole and multipole matrix elements (4).

Even then the first approximation is made in the perturbation theory calculation of Section 1.

For the statistical model we require more information than this but it is of a simpler nature and can be found from some simple fairly low resolution spectroscopic experiments of the type mentioned in Section 6. These experiments would be required at different temperatures. Each set of results would be required to satisfy the statistical model, which can then be used to determine the parameters given on page 60 as a function of temperature. The model then gives us an empirical formula for the absorption

$$A = A\left[p,\ \ell,\ \omega,\ \frac{S}{\alpha}(\omega,\ T),\ \frac{S}{d}(\omega,\ T)\right] \quad .$$

Of course this is for pure Lorentz lines. However, for shock-tube work of fairly short geometric path length, the pressure will need to be large enough to eliminate Doppler broadening effects in order to get a reasonable amount of emission.

If one method is carried right through to predicting A say, as above, then the other method can in principle be fitted to the empirical function A, and the required spectroscopic knowledge can be obtained for the fundamental method.

The spectral-model approach is a very common one, those mentioned in Section 4 (c) being a sample of the more sophisticated type.

The full set of models are:-

(i) The Box Approximation or Box-Model

This involves the definition of an effective bandwidth $\Delta\omega_{nn'}$, together with an average absorption coefficient $\bar{A}$. The result is that the absorption profile is considered to be of constant height, with vertical sides, having the same area as the measured absorption. The integrated band intensity (see Section 3(b).) leads directly to this model as soon as the band is given a width, which is arbitrarily defined for this model.

(ii) The "Just-Overlapping" Model

Here the average absorption coefficient is approximated by $(\frac{S_\omega}{d_\omega})$ and is considered a function of ω, where d_ω is the local line spacing. The range of validity is roughly the same as (i) but may be somewhat superior for moderate pressures and optical path length. The analysis is more complicated but leads to an unambiguous value of effective bandwidth.

(iii) Non-Overlapping Lines with Lorentz-Type Lines

For this model the analysis is as accurate as for a single line, but is available only for low temperatures and high resolution applications and is not applicable to the highly populated infrared bands of carbon dioxide.

(iv) Non-Overlapping Lines with Pure Doppler Broadening

As for (iii) but at high temperatures and low pressures.

(v) Non-Overlapping Lines with Mixed Lorentz-Doppler Broadening

This leads to a full range of temperature and pressure application - but only for high resolution.

(vi) The Elsasser Model

Equally spaced and equally intense spectral lines with arbitrary overlapping, and either of the two main line shapes.

(vii) The Statistical Model

Lines governed by random probability distributions for intensity and position in the band.

(viii) Random-Elsasser Model

A combination of (vi) and (vii), such that a complete Elsasser band becomes treated like one line in the pure statistical model.

(ix) Partially overlapping spectral lines with Doppler-broadening.

(x) A locally-applied statistical model for arbitrary over-lapping

and with pressure broadening. This amounts to considering equivalent width as a function of wavenumber, as in Sections 5 and 6.

It should be pointed out that the fundamental method of attack on the problem is also forced to become a model approach since we cannot predict the intra-molecular parameters precisely. In this case the expression for the band is that of a molecular model, for example, the harmonic oscillator model, rather than a less realistic spectral model which does not consider why the lines are there at all.

Spectral models were introduced and investigated mainly as a scape-goat at macroscopic level, because molecular models were too simple to predict realistic spectra, or too complicated to handle at all.

However, the method of Malkmus & Thomson (21) utilizes both a spectral and a molecular model and produces results which agree with experimental data. This is no doubt the best method of solution of the problem so far devised, but improvement on its accuracy while keeping the basic method the same would require algebraic solutions of higher order equations.

This work is part of a thesis presented to the University of Manchester in support of an application for the degree of M.Sc., in September 1965. I am grateful to Dr. H. K. Zienkiewicz for his active interest and encouragement in the preparation of this work, and to Mr. E. Wild for his helpful discussions on difficult theoretical points.

I am indebted to the Scientific Research Council for a maintenance grant during the compilation of this work.

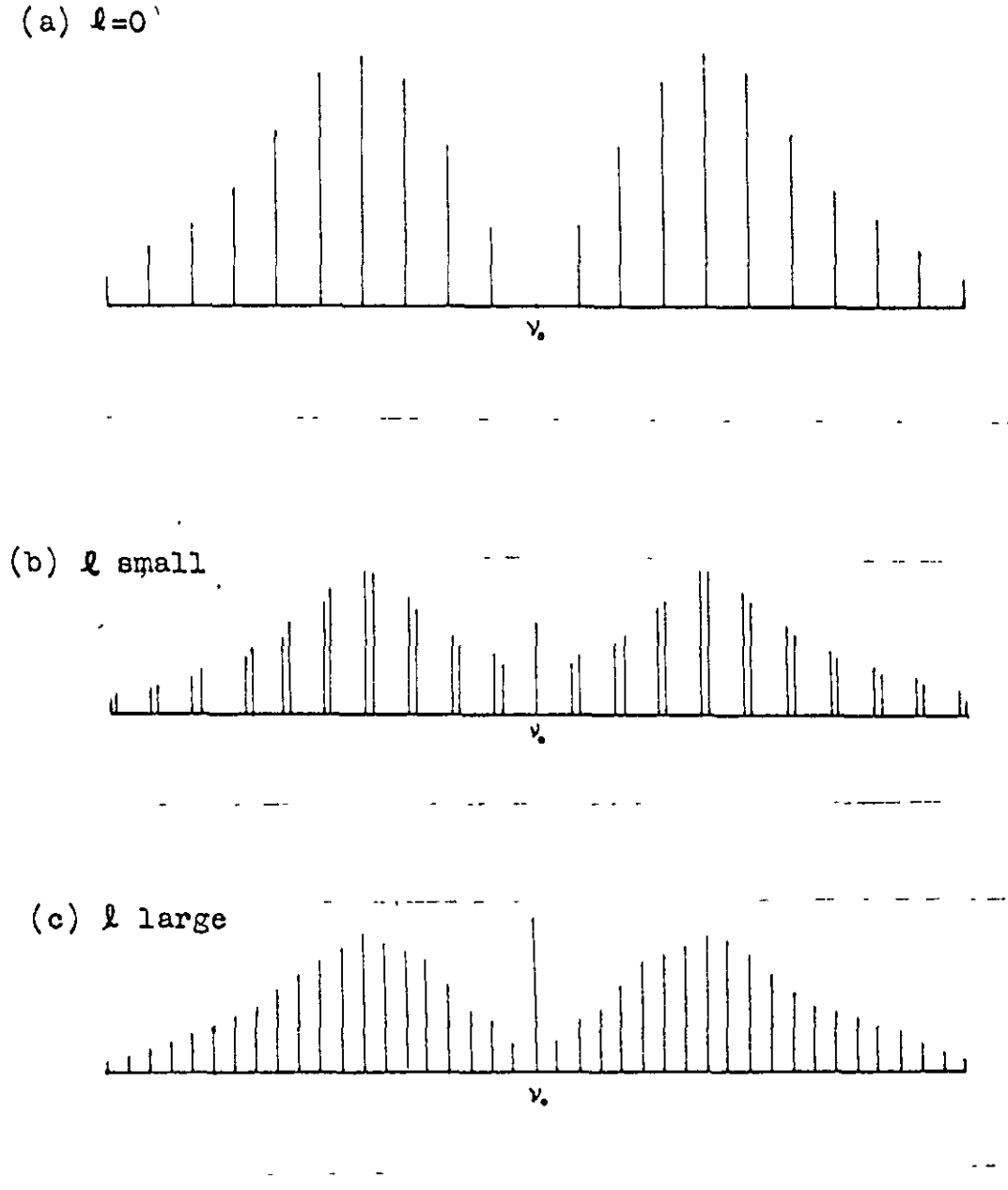

Fig.1.

Theoretical spectral line positions and relative intensities for typical component bands of the carbon dioxide 4.3μ band.

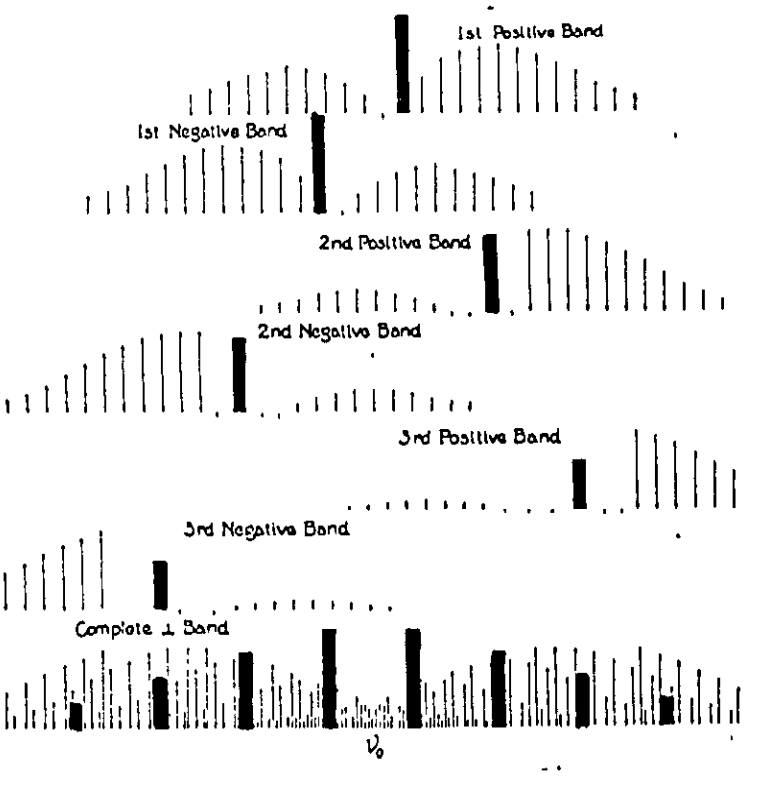

Fig. 1(d)

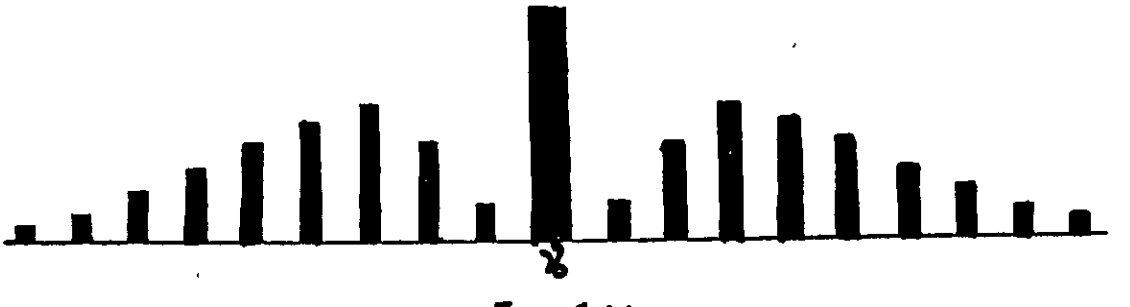

Fig. 1(e).

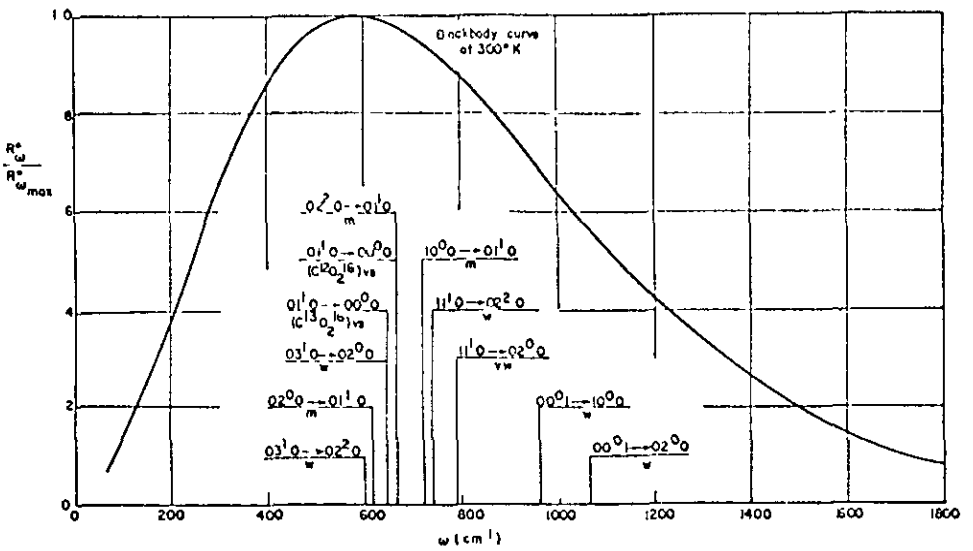

Fig. 2 (a)

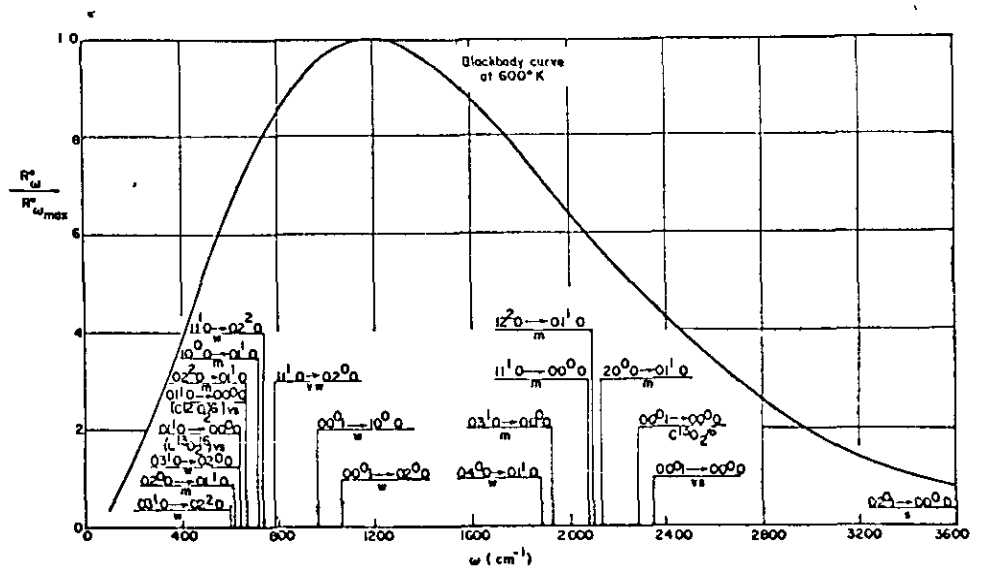

Fig. 2 (b)

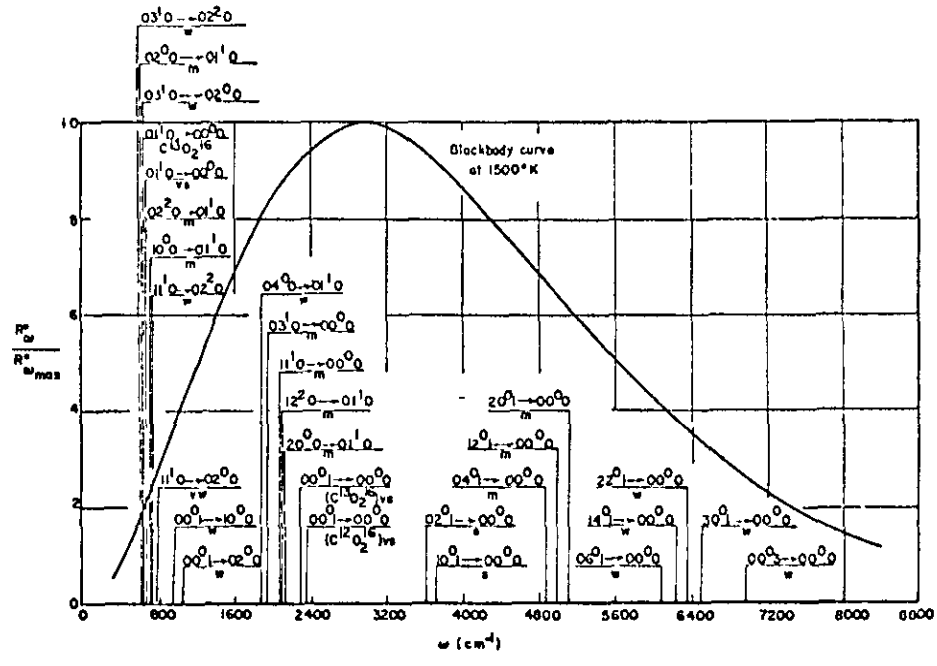

Fig. 2 (c)

Positions of centres of vibration-rotation bands observed at room temperature. The designations vs (very strong), s (strong), etc. are those of Herzberg (10) and correspond to those of the first column in Table 2. Also shown is the radiacy ratio ($R^{o}_{\omega}/R^{o}_{\omega max}$) for a blackbody at 300°K (2 (a)), 600°K (2(b)), and 1500°K (2 (c)).

Table 2.

Infrared Bands of Carbon Dioxide.

Band Type	Upper state		Lower state		calculated wavenumber (cm^{-1})	observed wavenumber (cm^{-1})	wavelength (microns)	
⊥ v.s.	01' 0	Π_u	00° 0	Σ^+_g	667.3*	667.3	14.98	⊙
⊥ m.	02° 0	Σ^+_g	01' 0	Π_u	618.1	618.5	16.17	⊙
⊥ m.	02² 0	Δ_g	01' 0	Π_u	668.1*	668.3	14.97	
⊥ m.	10° 0	Σ^+_g	01' 0	Π_u	720.8*	720.5	13.87	
⊥ w.	03' 0	Π_u	02² 0	Δ_g	596.5	596.8	16.76	
⊥ w.	03' 0	Π_u	02° 0	Σ^+_g	646.1	647.6	15.44	⊙
⊥ w.	11' 0	Π_u	02² 0	Δ_g	741.7	740.8	13.50	
⊥ vw.	11' 0	Π_u	02° 0	Σ^+_g	791.3	790.8	12.65	
⊥ w.	04° 0	Σ^+_g	01' 0	Π_u	1880.1	1886	5.302	
⊥ m.	12² 0	Δ_g	01' 0	Π_u	2094.9	2094	4.776	
⊥ m.	20° 0	Σ^+_g	01' 0	Π_u	2131.5	2137	4.679	
⊥ m.	03' 0	Π_u	00° 0	Σ^+_g	1931.9*	1932.5	5.175	
⊥ m.	11' 0	Π_u	00° 0	Σ^+_g	2077.1*	2076.5	4.816	
∥ $C^{13}O^{16}_2$	00° 1	Σ^+_g	00° 0	Σ^+_g		2284.5	4.377	
∥ v.s.	00° 1	Σ^+_g	00° 0	Σ^+_g	2349.4*	2349.3	4.257	⊙
∥ s.	02° 1	Σ^+_g	00° 0	Σ^+_g	3613.2	3609	2.771	
∥ s.	10° 1	Σ^+_g	00° 0	Σ^+_g	3715.6	3716	2.691	
∥ m.	04° 1	Σ^+_g	00° 0	Σ^+_g	4852.5	4860.5	2.057	⊙
∥ m.	12° 1	Σ^+_g	00° 0	Σ^+_g	4981.4*	4983.5	2.007	⊙
∥ m.	20° 1	Σ^+_g	00° 0	Σ^+_g	5104.3	5109	1.957	⊙
∥ w.	06° 1	Σ^+_g	00° 0	Σ^+_g	6074.5	6077	1.646	⊙
∥ w.	14° 1	Σ^+_g	00° 0	Σ^+_g	6231.4	6231	1.605	⊙
∥ w.	22° 1	Σ^+_g	00° 0	Σ^+_g	6354.4	6351	1.575	⊙
∥ w.	30° 1	Σ^+_g	00° 0	Σ^+_g	6518.9	6510	1.536	⊙
∥ w.	00° 3	Σ^+_g	00° 0	Σ^+_g	6973.1	6976	1.433	⊙
∥ v.w.	02° 3	Σ^+_g	00° 0	Σ^+_g	8192.9	8193	1.221	
∥ v.w.	10° 3	Σ^+_g	00° 0	Σ^+_g	8295.3	8293	1.206	
∥ v.w.	00° 5	Σ^+_g	00° 0	Σ^+_g	11496.5*	11496.5	0.8698	
∥ v.w.	02° 5	Σ^+_g	00° 0	Σ^+_g	12672.4*	12672.4	0.7891	
∥ v.w.	10° 5	Σ^+_g	00° 0	Σ^+_g	12774.7*	12774.7	0.7828	

* Used as standards to calculate other wavenumbers.

⊙ Shown in Fig.3, indicated by ↓ .

Bands bracketted together are in resonance.

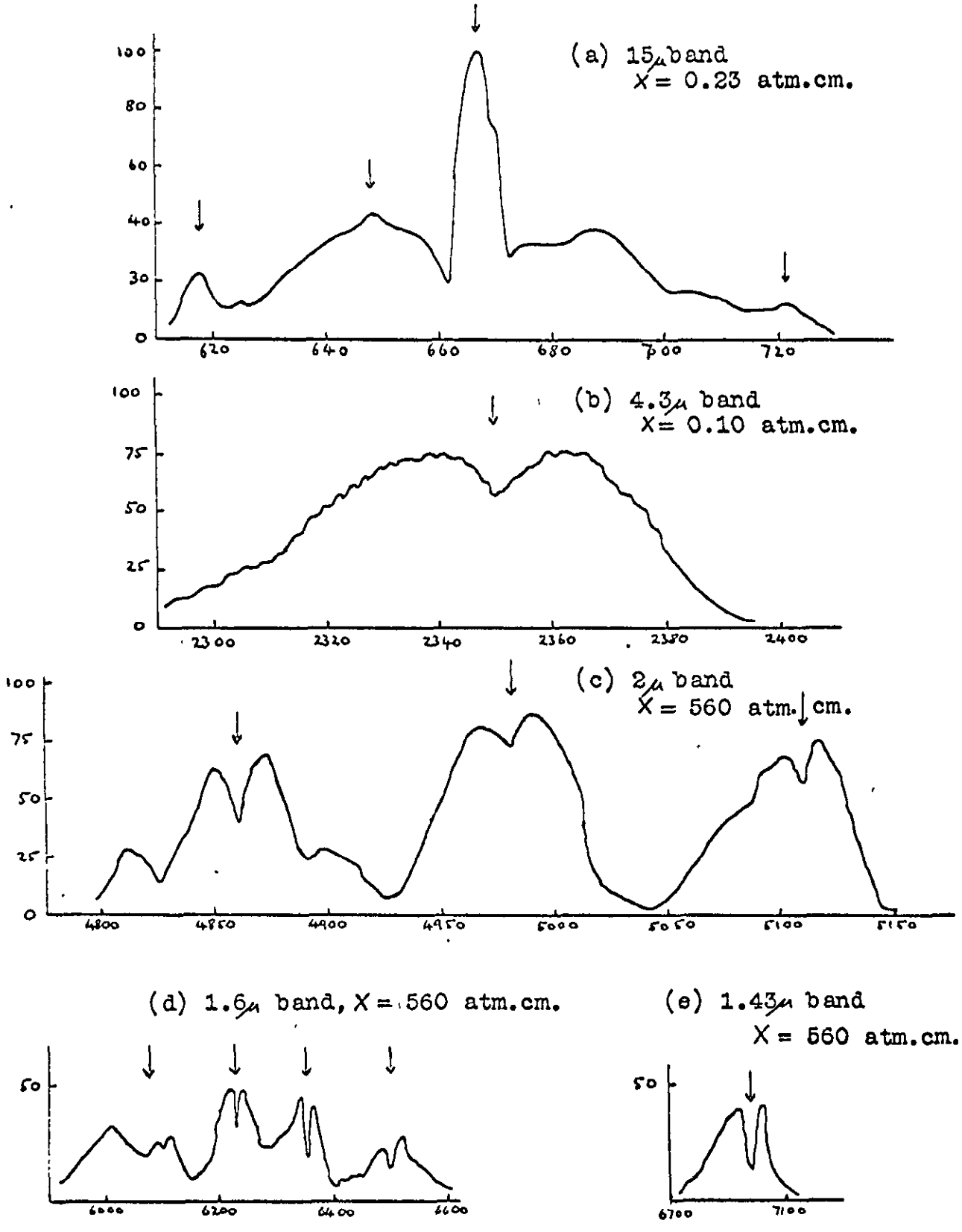

Fig.3.

Percentage absorptions of some bands of CO_2 at room temperature under low resolution.

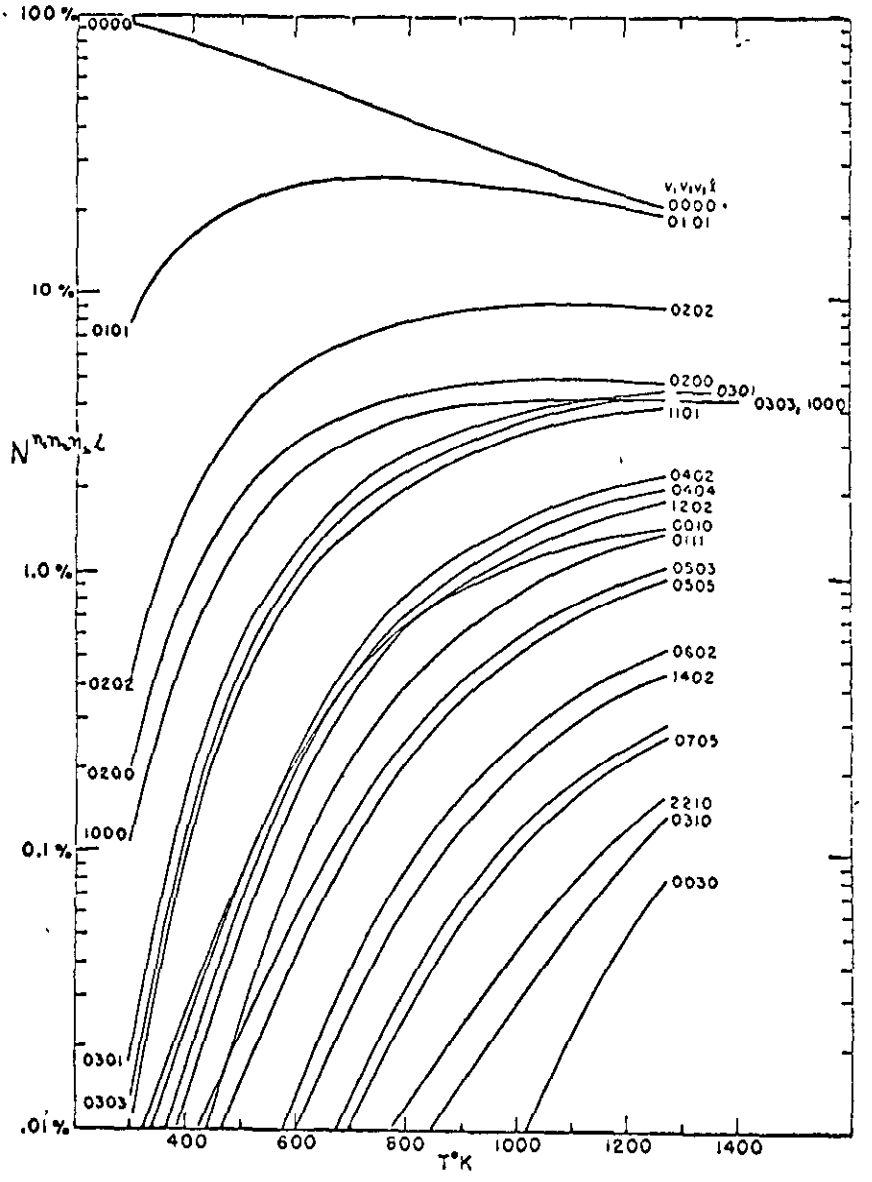

Fig.4.

Vibrational level populations of CO_2.

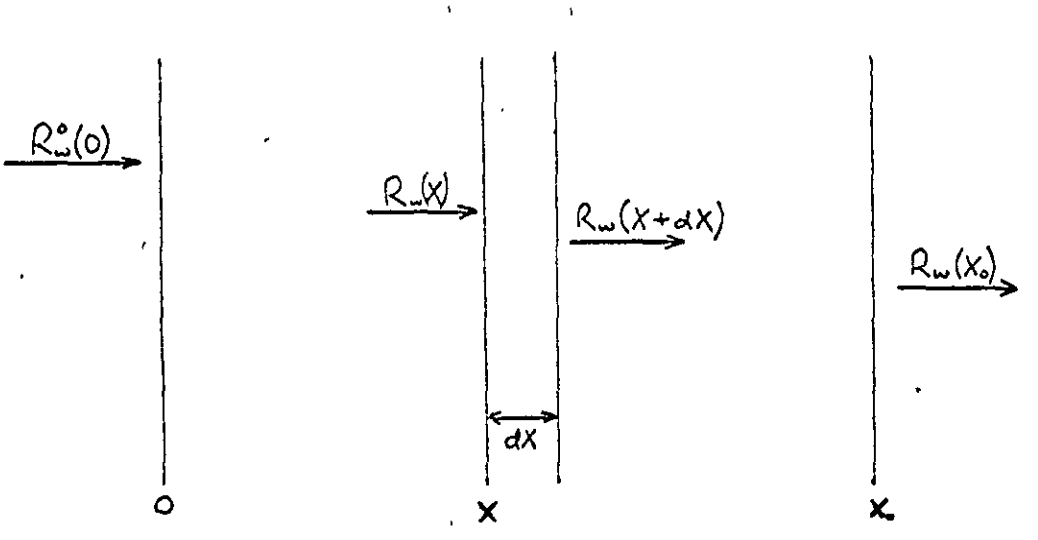

Fig. 5.

The intensity distribution of a spectral line with
(a) pure Lorentz broadening,
(b) pure Doppler broadening
for lines of unit integrated intensity, and identical half-widths.

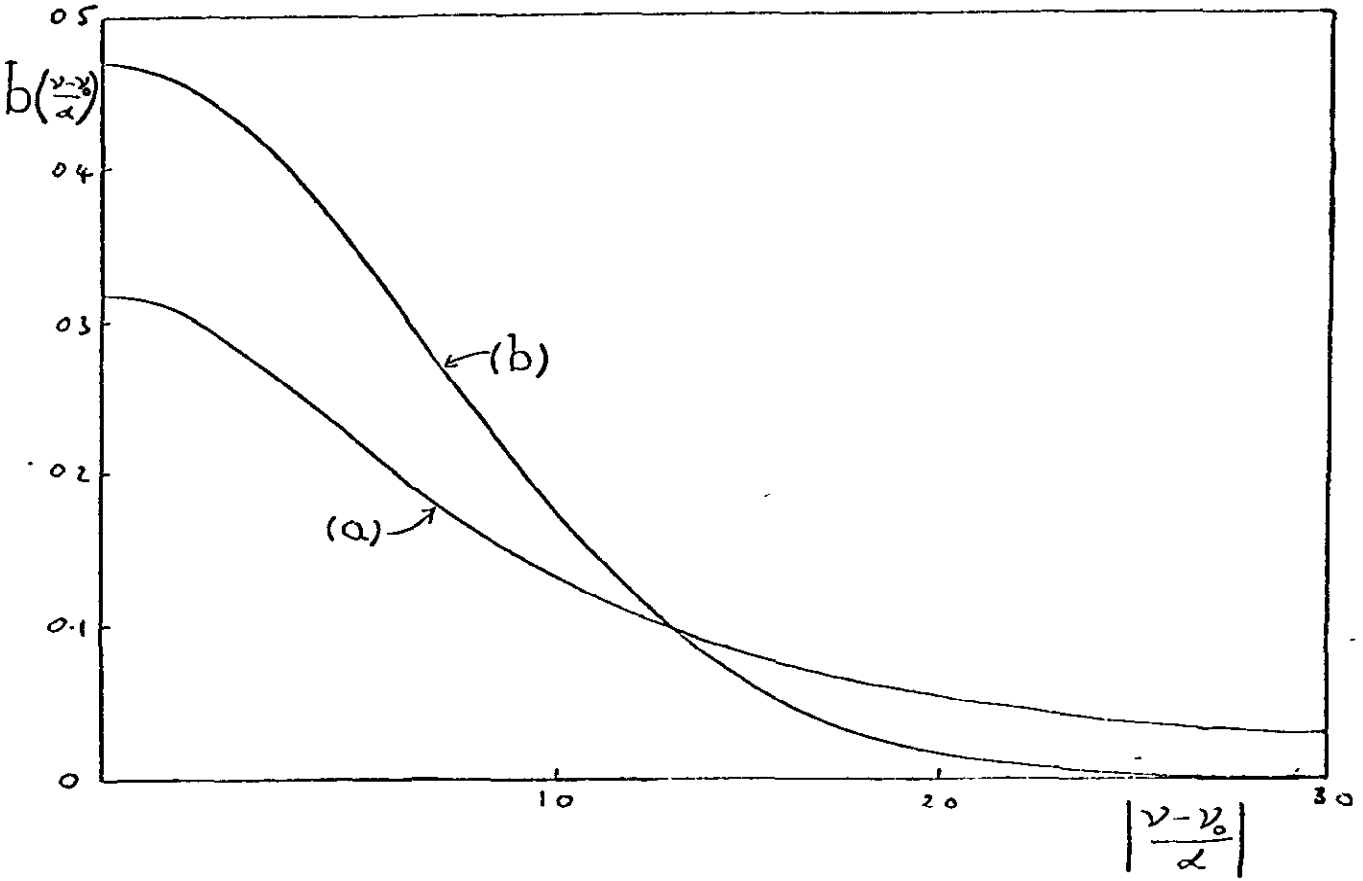

Fig.6.

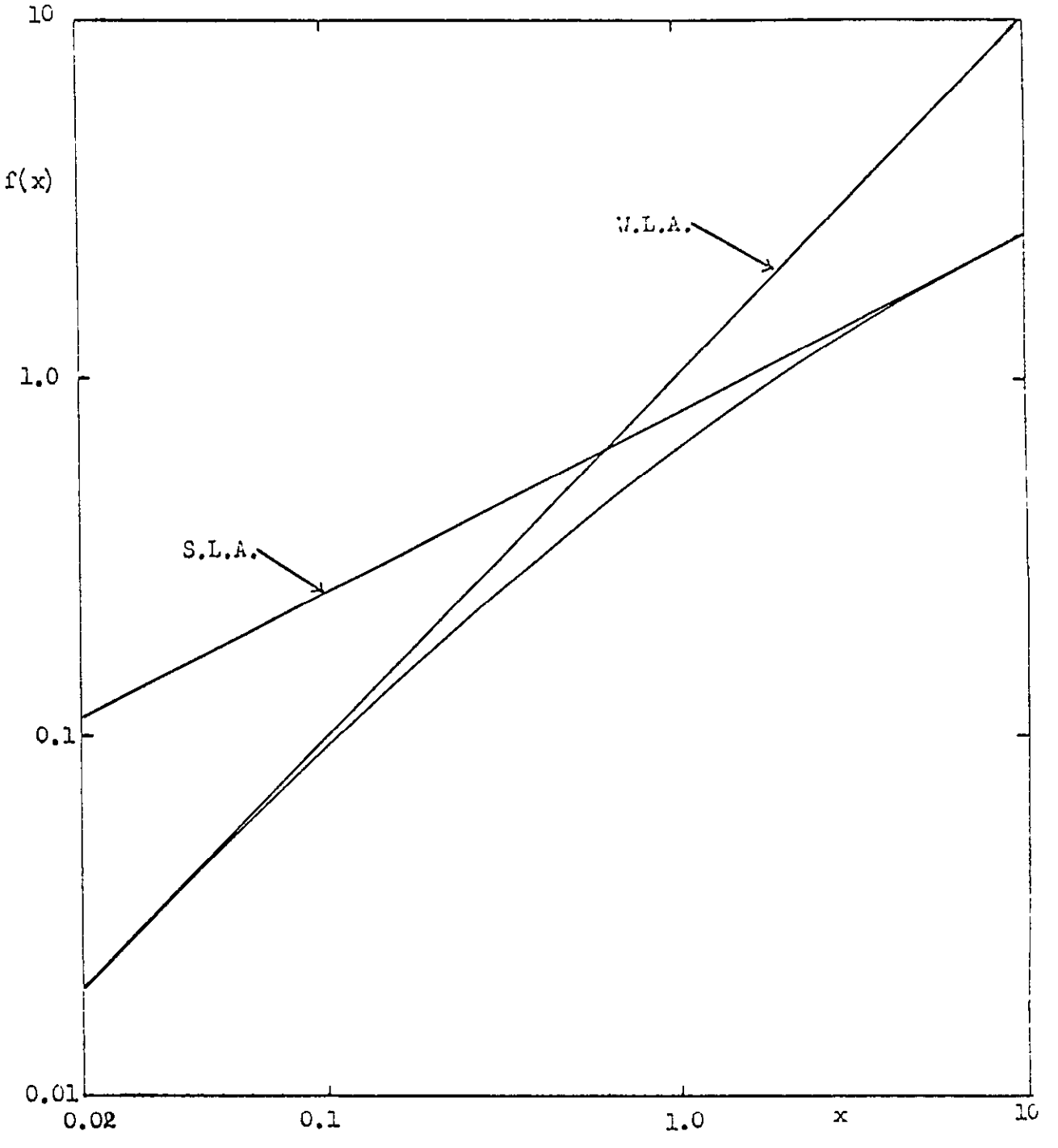

Fig. 7. The Ladenburg-Reiche Curve and W.L.A. and S.L.A.

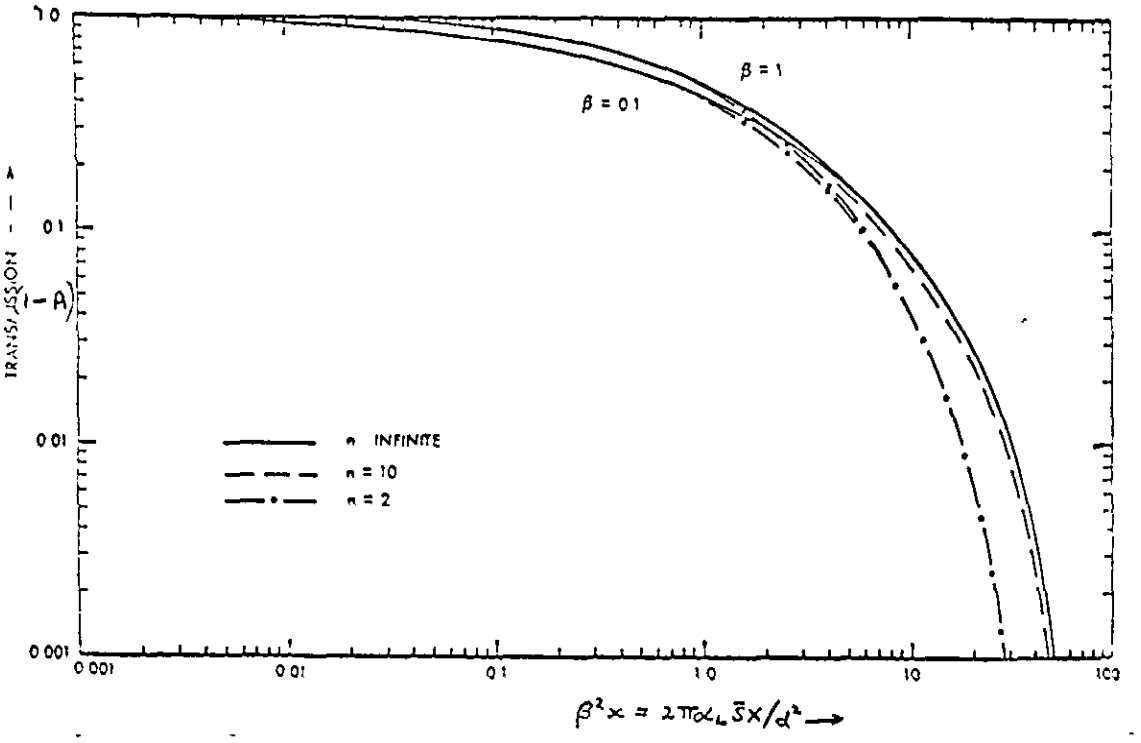

Fig. 8. Transmission for the statistical model of a band. It is assumed that all spectral lines are equally intense and that the Lorentz line shape is valid. 'n' represents the number of lines with random spacing, but the same mean spacing 'd' in each.

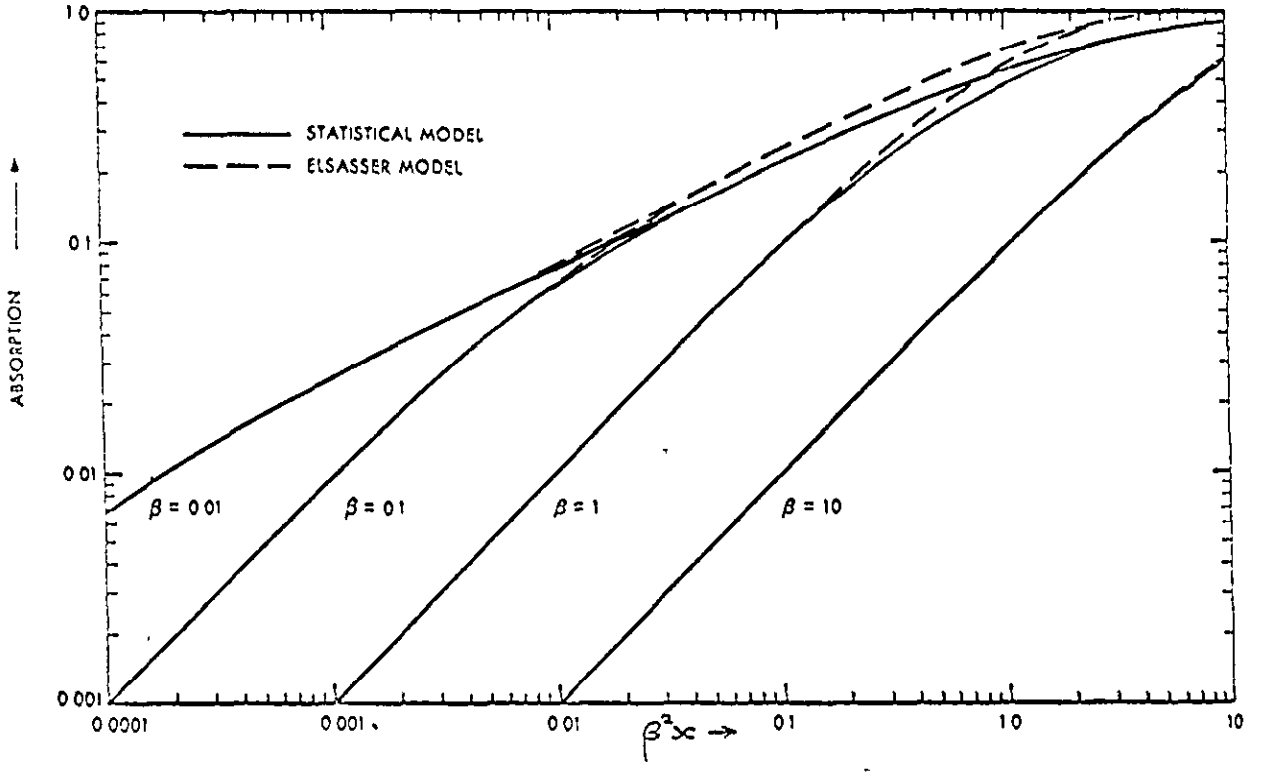

Fig. 9. Absorption for the statistical and Elsasser models of a band, assuming equally intense Lorentz lines.

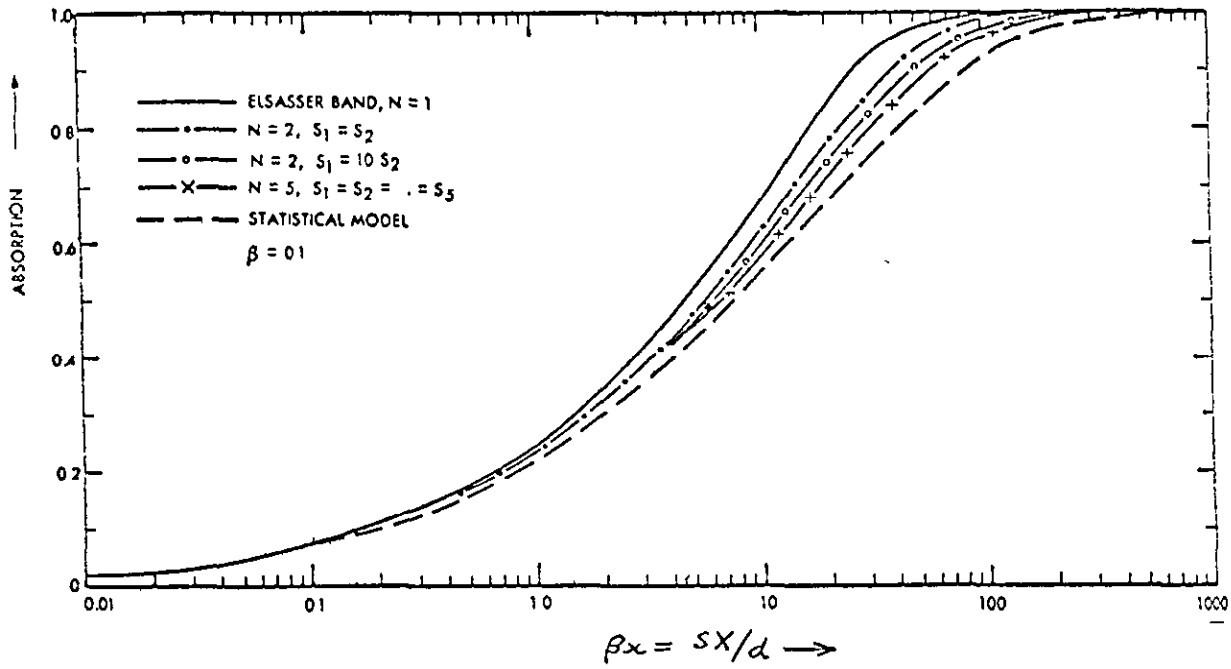

Fig. 10. Absorption as a function of $\beta x = SX/d$ for $\beta = 0.1$. The absorption is shown for a single Elsasser band (N=1); the random superposition of two Elsasser bands (N=2) where the intensities are equal ($S_1 = S_2$) and where one band is ten times as intense as the other ($S_1 = 10S_2$); the random superposition of five Elsasser bands (N=5) where the intensities in each band are equal ($S_1 = S_2 = \ldots = S_5$); the statistical model where all the intensities are equal.

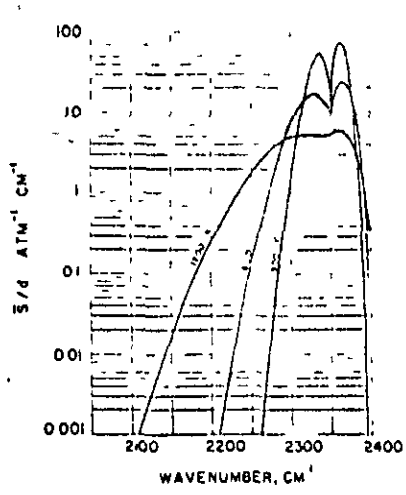

FIG 1 $\bar{S}/d$ vs wavenumber for T = 300°, 600°, and 1200°K

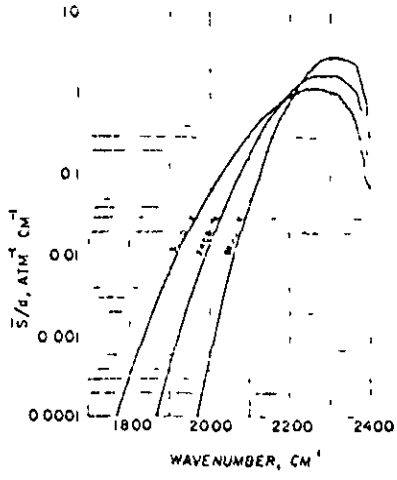

FIG 12 $\bar{S}/d$ vs wavenumber for T = 1500°, 2100°, and 3000°K

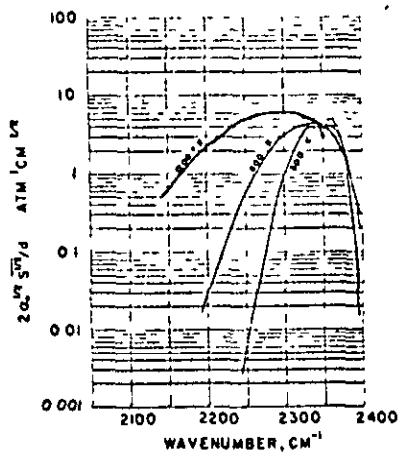

FIG 13 $2\alpha_0 b\bar{S}^{1/2}/d$ vs wavenumber for T = 300°, 600°, and 1200°K

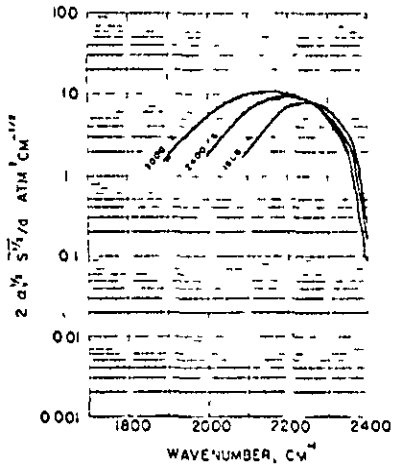

FIG 14 $2\alpha_0 b\bar{S}^{1/2}/d$ vs wavenumber for T = 1800°, 2400°, and 3000°K

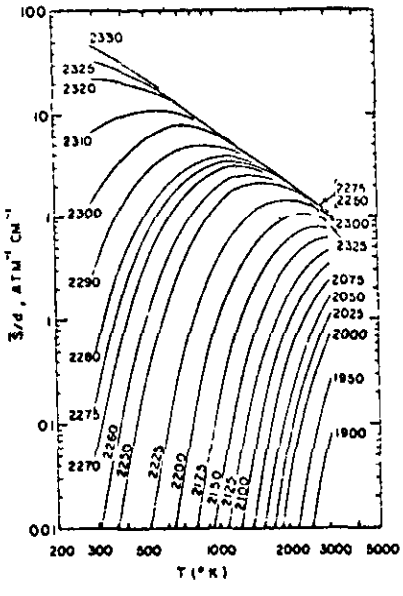

FIG 15 $\bar{S}/d$ vs T for $1900 \leq \omega \leq 2330$ cm^{-1}.

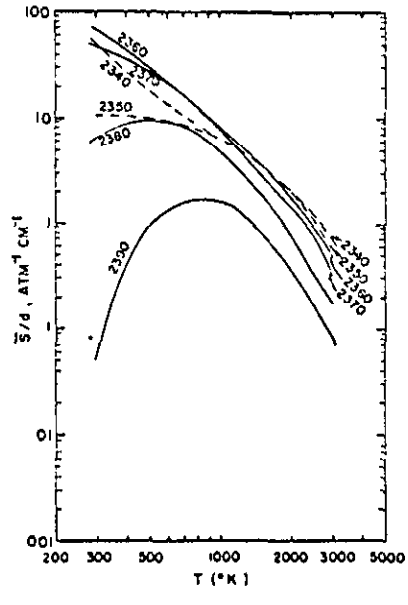

FIG 16 $\bar{S}/d$ vs T for $2340 \leq \omega \leq 2390$ cm^{-1}

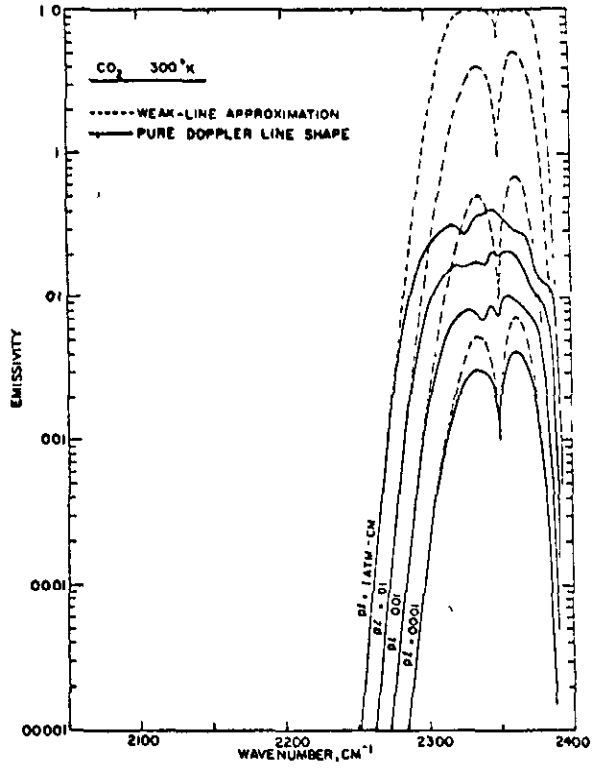

FIG 17. Emissivity vs wavenumber for pure Doppler line shape and weak-line approximation for $T = 300°K$.

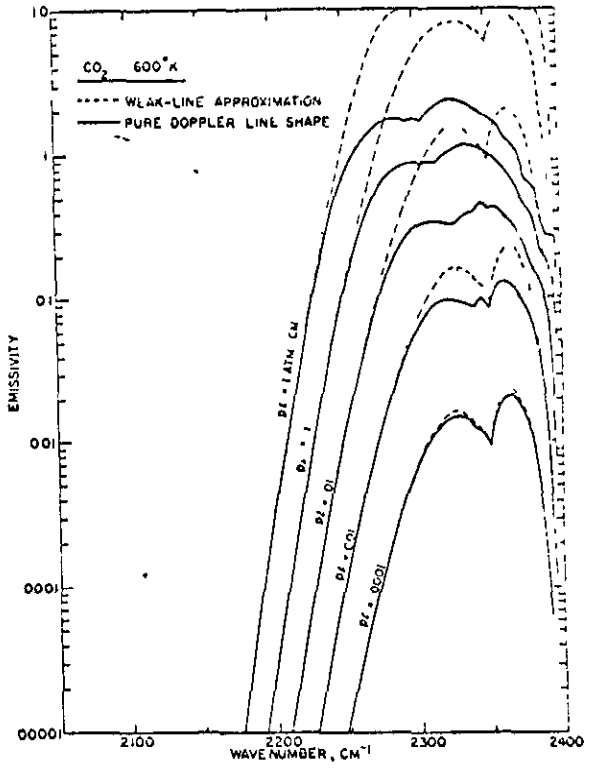

FIG. 18 Emissivity vs wavenumber for pure Doppler line shape and weak-line approximation for $T = 600°K$

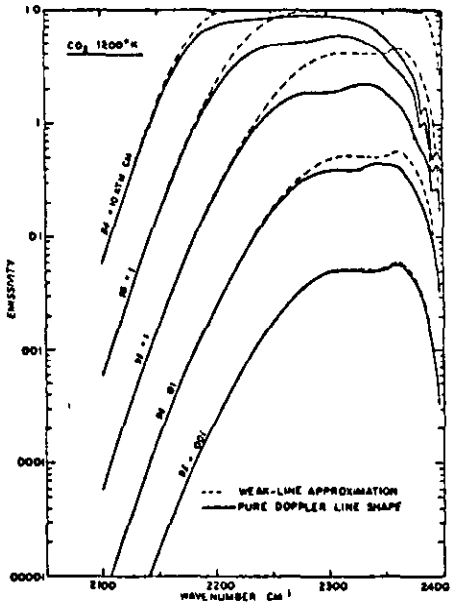

FIG 19 Emissivity vs wavenumber for pure Doppler line shape and weak-line approximation for $T = 1200°K$.

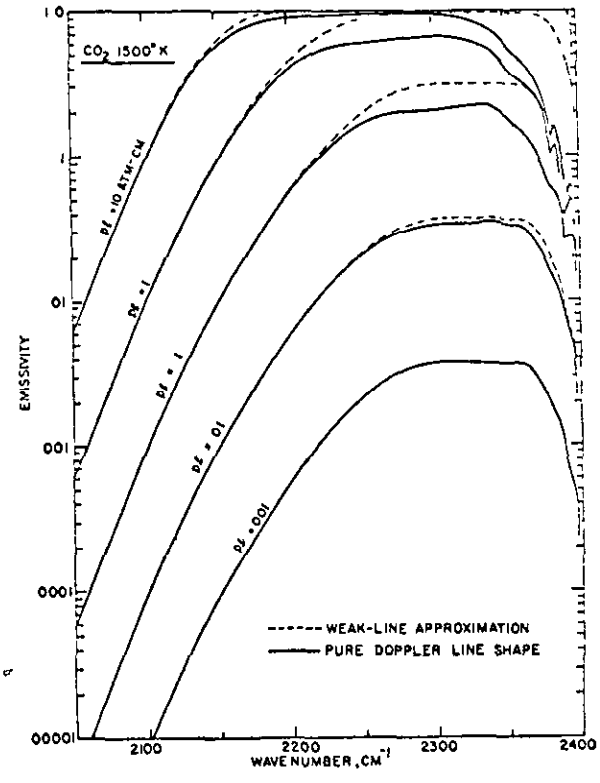

FIG. 20 Emissivity vs wavenumber for pure Doppler line shape and weak-line approximation for $T = 1500°K$

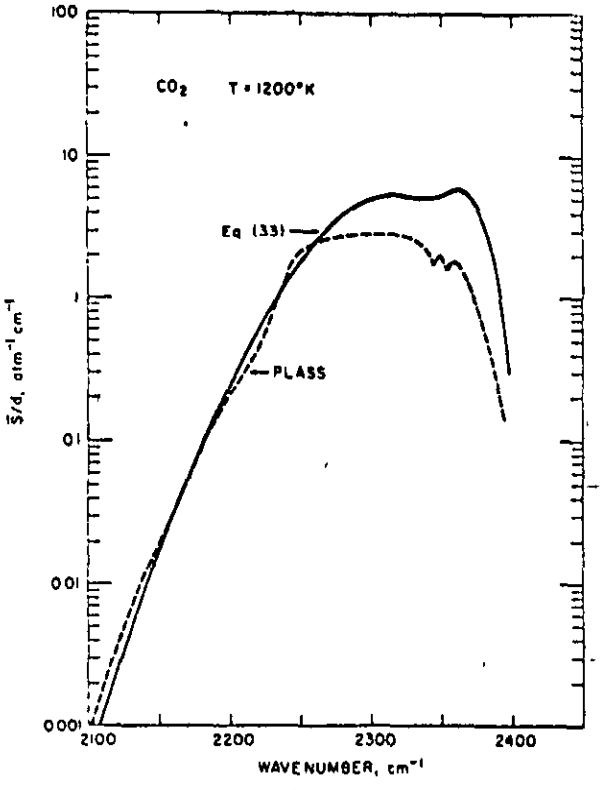

FIG. 21 Comparison of $\bar{S}/d$ with Plass at 1200°K

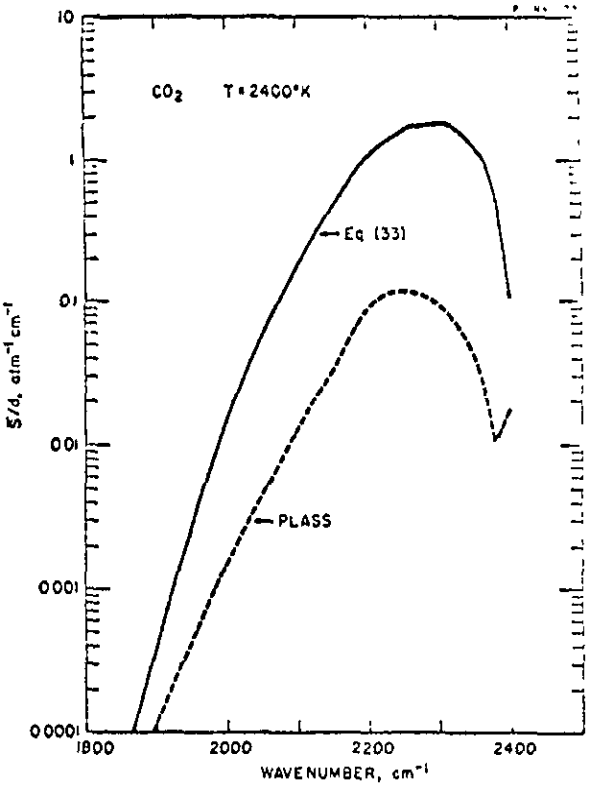

FIG. 22 Comparison of S/d with Plass at 2400°K.

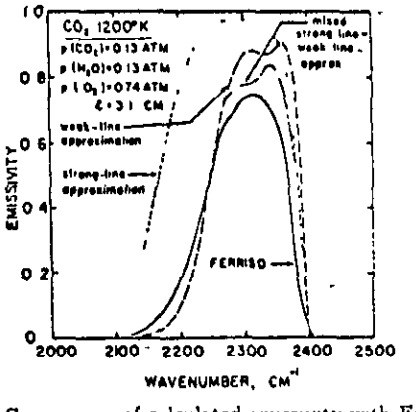

FIG 23 Comparison of calculated emissivity with Ferriso's measurements at 1200°K.

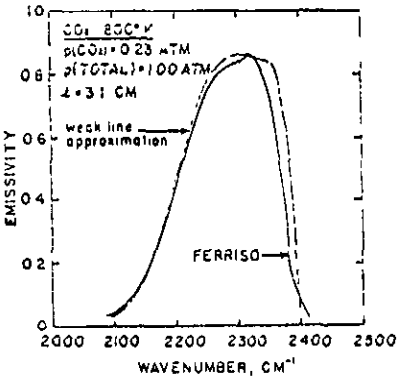

FIG. 24 Comparison of calculated emissivity with Ferriso's measurements at 1800°K

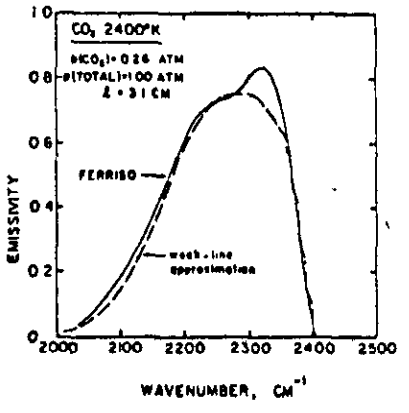

FIG. 25. Comparison of calculated emissivity with Ferriso's measurements at 2400°K.

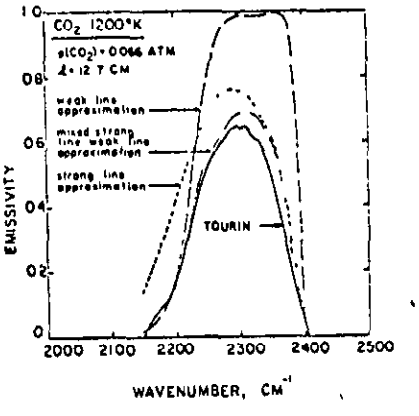

FIG. 26. Comparison of calculated emissivity with Tourin's measurements of pure CO_2 at 1200°K.

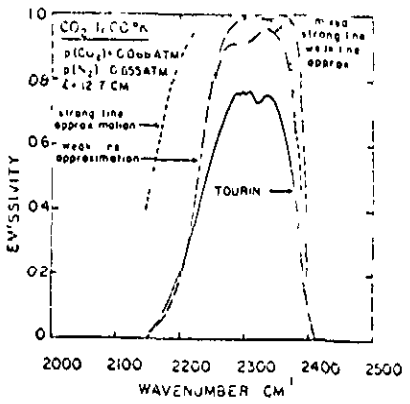

FIG 27 Comparison of calculated emissivity with Tourin's measurements of N_2 broadened CO_2 at 1200°K.

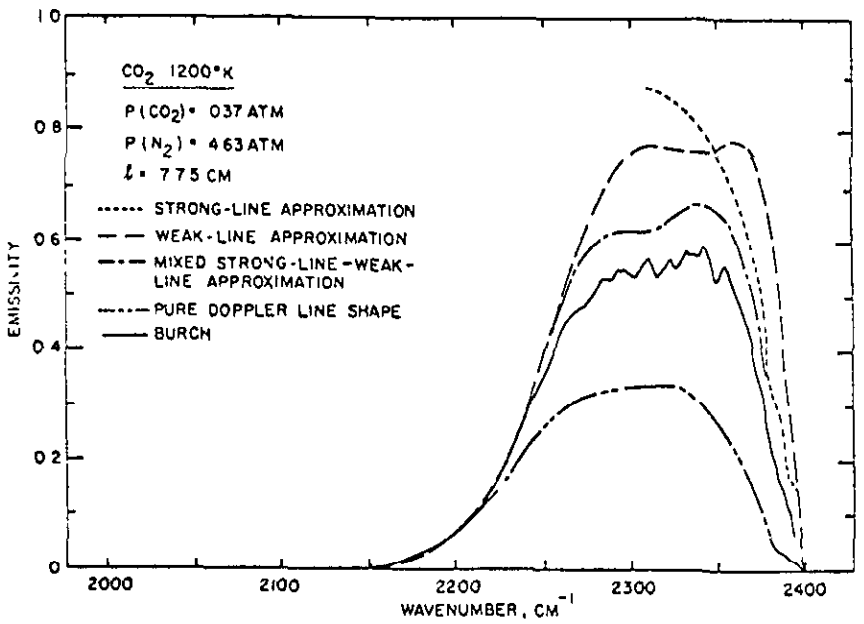

FIG 28 Comparison of calculated emissivity with Burch's measurements at 1200°K.

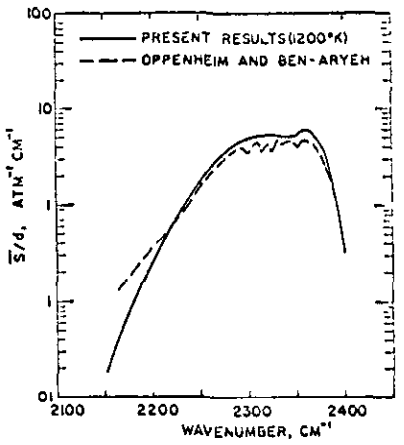

FIG 29 Comparison of $\bar{S}/d$ with Oppenheim and Ben-Aryeh's extrapolated experimental measurements

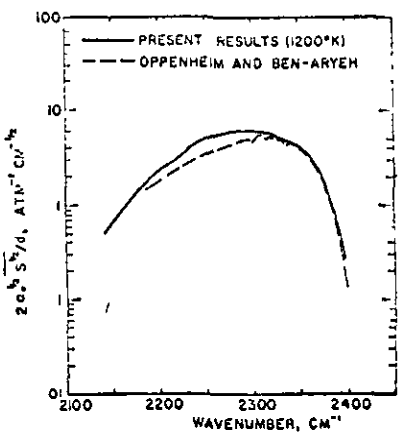

FIG 30 Comparison of $2\alpha_0^{\frac{1}{2}}\bar{S}^{\frac{1}{2}}/d$ with Oppenheim and Ben-Aryeh's extrapolated experimental measurements.

The Ladenburg-Reiche plot compared with experimental results and the weak and strong line approximations.

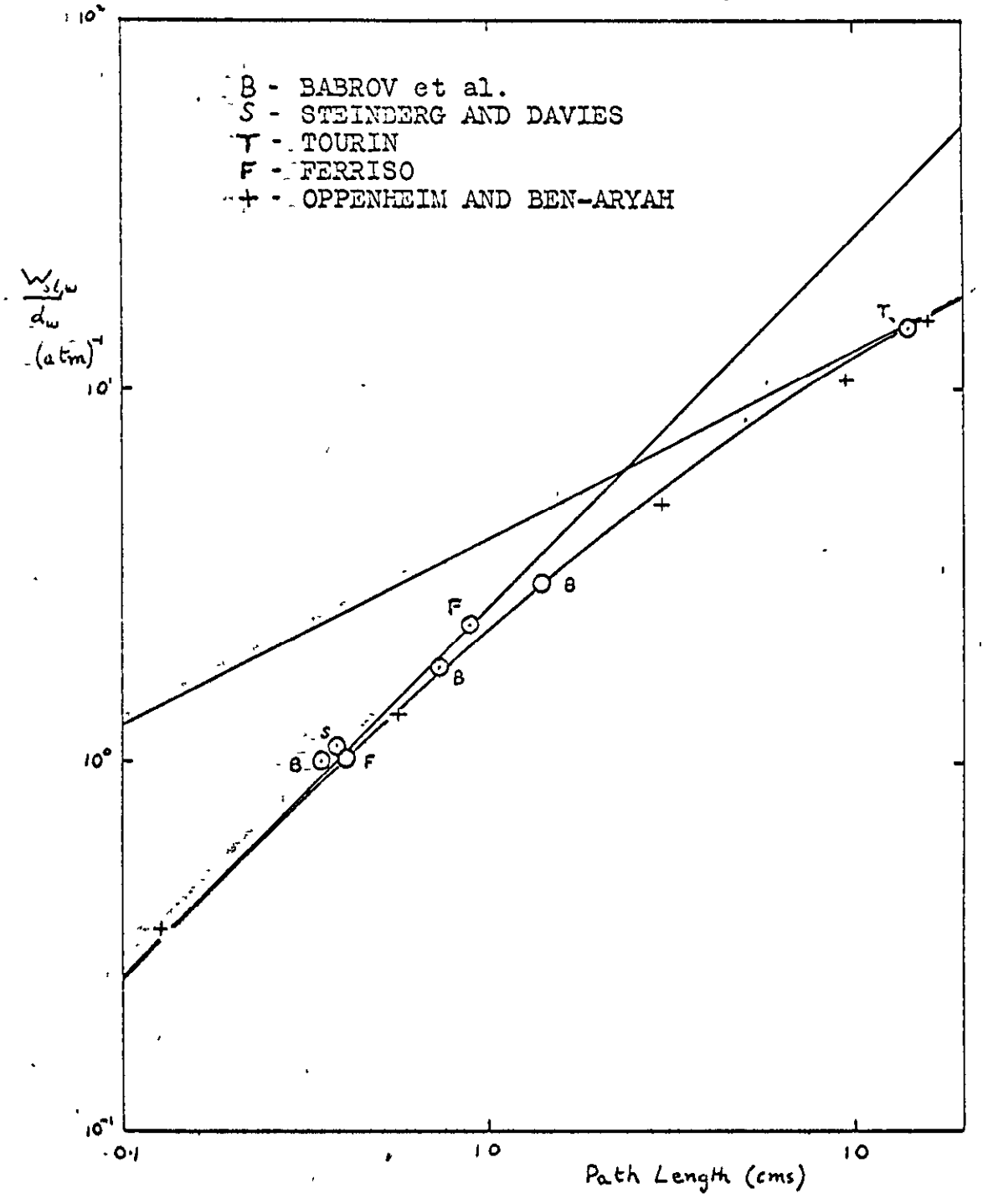

Fig.31.

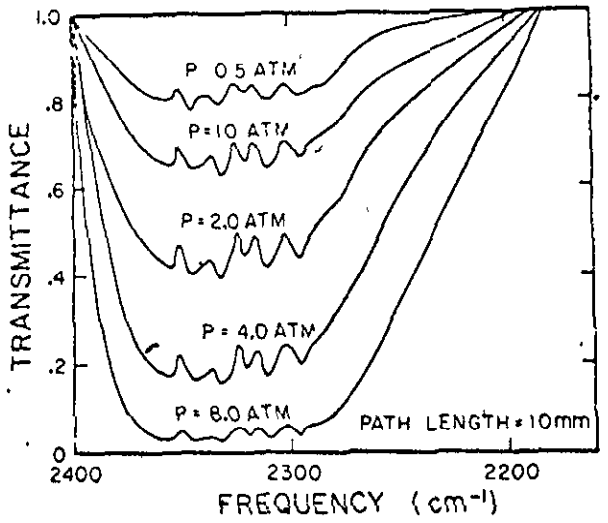

(a)

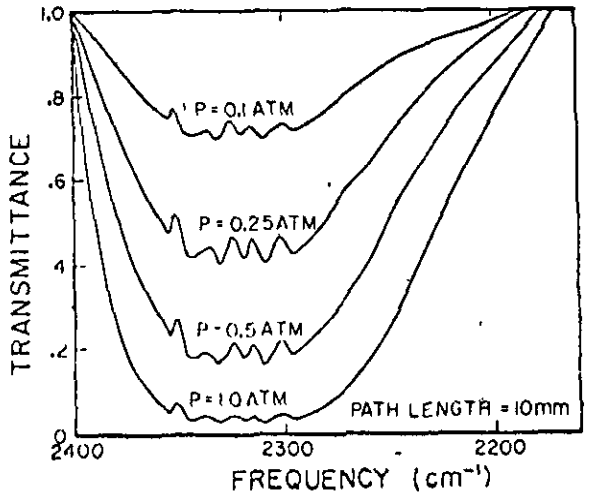

(b) Fig.32.

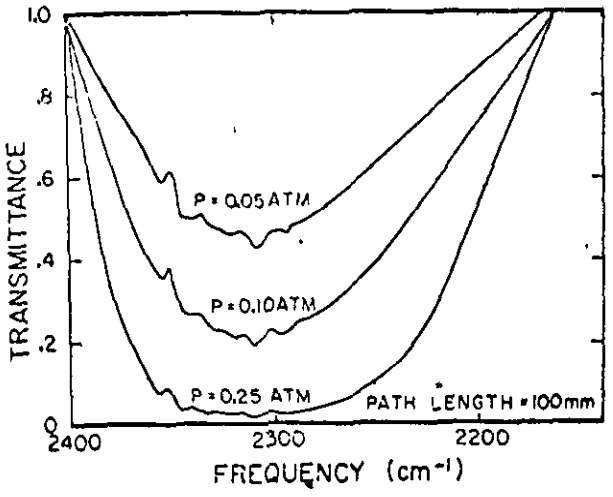

(c)

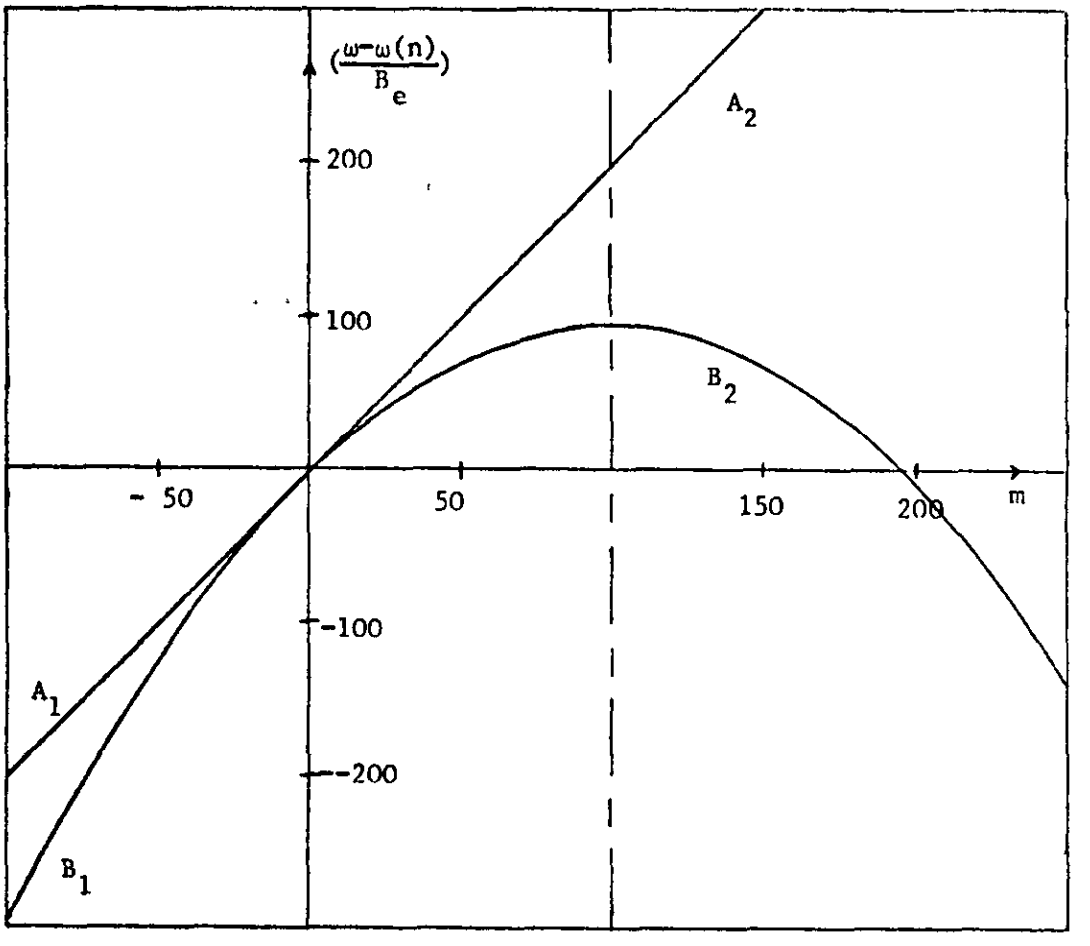

Fig. 33.

A plot of $(\frac{\omega-\omega(n)}{B_e})$ versus m (Equ. 5.3).

Curve A_1A_2 represents the case for α_e=0, curve B_1B_2 represents the case for α_e=0.01 B_e (typical) and n=1. The vertical line m=0 divides the P-branch from the R-branch, but the vertical line m=99 divides the two solutions obtained by Malkmus and Thomson (21). It can be seen that the solution for m>99 represents the region where the first order interaction term has become the dominating one. Also, we can see that the solution for m<99 represents both the P- and R-branches. Since the integrated line intensity of lines with m>99 is very small this solution has a negligible effect on the final value of the emissivity.

B I B L I O G R A P H Y

1. S. S. Penner
"Quantitative Molecular Spectroscopy and Gas Emissivities"
Pergamon Press, 1959.

2. Powell and Craseman,
"Quantum Mechanics", Addison-Wesley, 1962

3. Heitler,
"The Quantum Theory of Radiation", Clarendon Press,
Oxford, 1954.

4. Blatt and Weisskopf,
"Theoretical Nuclear Physics", John Wiley and Sons, 1952.

5. D. M. Dennison,
Rev. Mod. Phys. 3, 280 (1931)

6. R. C. Herman and K. E. Shuler,
J. Chem. Phys. 22, 481 (1954)

7. R. C. Herman and R. F. Wallis,
J. Chem Phys. 23, 637 (1955)

8. H. Hanson, H. H. Nielsen, W. H. Shaffer and J. Waggoner,
J. Chem Phys. 27, 40 (1957)

9. D. M. Dennison,
Ref. Mod. Phys. 12, 175 (1940)

10. G. Herzberg,
"Infrared and Raman Spectra", Van Nostrand, (1962)

11. E. U. Condon and G. H. Shortley,
"The Theory of Atomic Spectra", Cambridge University
Press, (1951)

12. H. Hanson, et al.
J. Chem. Phys. 27, 40 (1957)

13. W. Malkmus
J. Opt. Soc. Am. 53, 951 (1963)

14. R. H. Tourin,
J. Opt. Soc. Am. 51, 175 (1961)

15. "Planck Radiation Functions and Electronic Functions",
Federal Works Agency, WPA, Nat. Bur. Standards,
Washington D.C. (1941)

16. M. Zemansky,
"Heat and Thermodynamics", McGraw-Hill, 1957.

17. G. N. Plass,
J. Opt. Soc. Am. 48, 690 (1958)

18. R. Ladenburg and F. Reiche,
Ann.Physik. 42, 181 (1913).

19. G. N. Plass and D. I. Fivel,
Astrophys. J. 117, 225 (1953)

20. W. M. Elsasser,
Phys. Rev. 54, 126 (1938)

21. W. Malkmus and A. Thomson,
J. Quant. Spectry. and Rad. Transfer 2, 17 (1962).
Also: Convair Report ZPh-095, "Infrared Emissivity of Diatomic Gases for the Anharmonic Vibrating Rotator Model", May, 1961; and Convair Report ZPh-119, "Infrared Emissivity of Diatomic Gases with Doppler Lineshape", Sept. 1961.

22. C. P. Courtoy,
Can. J. Phys. 35, 608 (1957)

23. W. S. Benedict and E. K. Plyler,
"High-Resolution Spectra of Hydrocarbon Flames",
Nat. Bur. Standards Circ. No. 523, p.p. 57-73, 1954.

24. L. D. Kaplan and D. F. Eggers,
J. Chem Phys. 25, 876 (1956)

25. U. P. Oppenheim and Y. Ben-Aryah,
J. Opt. Soc. Am. 53, 344 (1963).

26. W. S. Benedict, R. C. Herman, G. E. Moore and S. Silverman,
Can. J. Phys. 34, 830 (1956)

27. G. N. Plass,
J. Opt. Soc. Am. 49,821 (1959)

28. C. C. Ferriso,
J. Chem. Phys. 37, 1955 (1962).

29. D. E. Burch and D. A. Gryvnak,
"Infrared Radiation Emitted by Hot Gases and its Transmission through Synthetic Atmospheres", Aeronutronic Report U-1929,;
Oct. 1962.

30. M. Steinberg and W. O. Davies,
J. Chem Phys. 34, 1375 (1961)

31. V. Stull and G. Plass
J. Opt. Soc. Am. 50, (1960)

Diagrams were taken from the following papers:

D. M. Dennison, Ref. 5, Fig. 1 (d)

S. S. Penner, Ref. 1. Fig. 2.

G. Herzberg, Ref. 10, Fig. 3, Table 2.

R. H. Tourin, Ref. 14, Fig. 4.

G. N. Plass, Ref. 17, Figs. 8, 9, 10.

W. Malkmus, Ref. 13, Figs. 11 to 30.

U. P. Oppenheim and Y. Ben-Aryah, Ref. 25, Figs. 31, 32.

A.R.C. C.P. No. 981
December, 1966
J. P. Hodgson

A SURVEY OF THE INFRARED RADIATION PROPERTIES OF CARBON DIOXIDE

This paper consists of a survey of theoretical and experimental approaches to the prediction of the low resolution emissivity of an infrared band of a polyatomic molecule. Spectral band models and molecular models are discussed, with carbon dioxide being taken as an example of such a molecule.

A.R.C. C.P. No. 981
December, 1966
J. P. Hodgson

A SURVEY OF THE INFRARED RADIATION PROPERTIES OF CARBON DIOXIDE

This paper consists of a survey of theoretical and experimental approaches to the prediction of the low resolution emissivity of an infrared band of a polyatomic molecule. Spectral band models and molecular models are discussed, with carbon dioxide being taken as an example of such a molecule.

A.R.C. C.P. No. 981
December, 1966
J. P. Hodgson

A SURVEY OF THE INFRARED RADIATION PROPERTIES OF CARBON DIOXIDE

This paper consists of a survey of theoretical and experimental approaches to the prediction of the low resolution emissivity of an infrared band of a polyatomic molecule. Spectral band models and molecular models are discussed with carbon dioxide being taken as an example of such a molecule.

Printed and published by
HER MAJESTY'S STATIONERY OFFICE

To be purchased from
49 High Holborn, London W C 1
423 Oxford Street, London W 1
13A Castle Street, Edinburgh 2
109 St Mary Street, Cardiff CF1 1JW
Brazennose Street, Manchester 2
50 Fairfax Street, Bristol 1
258–259 Broad Street, Birmingham 1
7–11 Linenhall Street, Belfast BT2 8AY
or through any bookseller

Printed in England

S O Code No 23-9017-8